Boundary Effects on a Thermophoretic Sphere in an Arbitrary Direction of a Plane Surface

Shih H. Chen
Dept. of Chemical Engineering, Hwa Hsia College of Technology and Commerce, Taipei 235, Taiwan

The thermophoresis of a sphere in a constant applied temperature gradient in an arbitrary direction with respect to a plane surface was analytically studied. The Knudsen number was assumed small to describe the fluid flow by a continuum model with a thermal creep and a hydrodynamic slip at the particle surface. The asymptotic formulas for the temperature and velocity fields in the quasi-steady situation were obtained by a method of reflections. The plane surface can be a solid wall or a free surface. The boundary effect on the thermophoretic motion was weaker than that on the motion driven by a body force. Even so, the interaction between the plane and particle can be very significant when the gap thickness gets small. For a particle motion normal to a solid wall, plane surface effect reduces the thermophoretic velocity of the particles; however, this solid wall may be an enhancement factor on the particle migration as it is translating parallel to the wall. On the other hand, in the case of a particle migrating close to a free surface due to thermophoresis, the particle velocity can be either greater or smaller than what would exist in the absence of the plane surface, depending on the relative thermal conductivity and surface properties of the particle and its relative distance from the plant. The thickness of the thermophoretic interacting region was also evaluated by considering the thermophoretic mobility. A free surface generally exerts less influence on the particle movement than does a solid surface.

Introduction

The thermophoretic motion describes the motion of aerosol particles in response to a temperature gradient, which was first described by Tyndall in 1870 (Waldmann and Schmitt, 1966; Bakanov, 1991). As is explained by the kinetic theory of gases (Kennard, 1938), the high-energy molecules in the hot region of the gas impinge on the particles with momenta greater than molecules coming from the cold region, thus leading to the migration of the particles in the direction opposite to the temperature gradient. Since thermophoresis is a mechanism for the capture of aerosol particles on the cold surfaces, it is of considerable importance in many practical applications, such as sampling of aerosol particles (Friedlander, 1977), modified chemical-vapor deposition (Weinberg, 1982), scale formation on the surface of heat exchangers (Montassier et al., 1991), microelectronic manufacturing (Ye et al., 1991), nuclear reactor safety (Williams and Loyalka, 1991), and cleaning of air (Sasse et al., 1994).

Assuming a small Knudsen number (l/a, where a is the radius of the particle and l is the mean free path of the gas molecules), Peclet number, and Reynolds number, as well as the effect of temperature jump, thermal creep, and hydrodynamic slip at the interface of the gas-particle, Brock (1962) has obtained the thermophoretic velocity of an aerosol sphere in a constant temperature gradient ∇T_∞ as

$$U^{(0)} = -\left[\frac{2C_s(k + k_i C_t l/a)}{(1+2C_m l/a)(2k + k_i + 2kC_t l/a)}\right]\frac{\eta}{\rho \bar{T}}\nabla T_\infty. \quad (1)$$

In Eq. 1, ρ, η, and k are, respectively, the density, viscosity, and thermal conductivity of the gas; k is the thermal conductivity of the particle; T is the bulk-gas absolute temperature at the particle center in the absence of the particle (or the mean gas temperature in the vicinity of the particle); C_s, C_t, and C_m are the dimensionless coefficients corresponding to the thermal creep, temperature jump, and hydrodynamic slip phenomena, respectively, at the particle surface and must be determined experimentally for each gas–solid system; $C_s = 1.17$, $C_t = 2.18$, and $C_m = 1.14$ are a set of reasonable kinetic-theory values for complete thermal and momentum accommodations (Talbot et al., 1980). Note that the negative sign in Eq. 1 indicates the particle migration in the direction of decreasing temperature, and $\rho \bar{T}$ is a constant for an ideal gas at constant pressure. Brock's (1962) analysis was extended to spheroid particles by using the prolate and oblate spheroidal coordinate systems (Leong, 1984). Considering both the thermophoretic and the gravitational effects, the migration of a single aerosol sphere was recently analyzed by Keh and Yu (1995).

In most real situations of thermophoresis, aerosol particles are not isolated and will move in the presence of neighboring particles. Recently, much progress has been made in the theoretical analysis concerning the applicability of Eq. 1 for an aerosol particle in a variety of bounded systems (Chen and Keh, 1995a, 1996; Keh and Chen, 1995, 1996a). Several important conclusions were made from these investigations of particle interactions in thermophoretic motion. First, the particle interaction effect on the thermophoresis is generally much weaker than that on the sedimentation that the hydrodynamic slip phenomenon permits at the particle–fluid interface. It is because the disturbance to the fluid velocity field caused by a thermophoretic sphere decays faster (as r^{-3}, where r is the distance from the particle center) than that caused by a settling particle (as r^{-1}). In sedimentation, the gravity induces a body force that is exerted on the particle and a nonzero hydrodynamic force balances this force. However, there is no hydrodynamic force exerted on the particle in thermophoretic motion. Thus, the disturbance flow fields in the two situation decays at a different rate with r. Second, in the case of two identical spheres aligned parallel to the prescribed temperature gradient, the effect of interaction makes each particle move faster than the velocity it would possess if isolated, while in the case of two identical spheres undergoing thermophoresis normal to their center line, each particle migrates slower than its undisturbed velocity. Third, the translating velocity of each coexistent identical thermally insulated particle, which can be arbitrarily oriented, is unaffected by the presence of the others. Fourth, the influence of interactions between particles is in general far greater on the smaller one than on the larger one.

Considering the influence of the boundary effect on particle velocity (or mobility), the movement of a thermophoretic particle perpendicular to a solid and/or a free surface was examined analytically by using a method of reflections (Chen, 1999). In the study, not only the particle mobility under the influence of boundary effects but also the deposition time of a particle translating through the thermophoretic boundary layer was evaluated. In general, a free surface exerts less influence on the particle movement than does a solid wall. The objective of the present study is to extend the previous work to the thermophoresis of an aerosol sphere moving in an arbitrary direction to a nearby surface. The infinite thermally conductive plane boundary can be either a solid wall or a free surface. The quasi-steady energy and momentum equations applicable to the system are solved by using a method of reflections. Moreover, the analytical results to correct Eq. 1 for various cases of flow are also presented in the study. It is found that the effect of the presence of the plane surface on the particle velocity can be significant when the gap between the particle and the plane gets small.

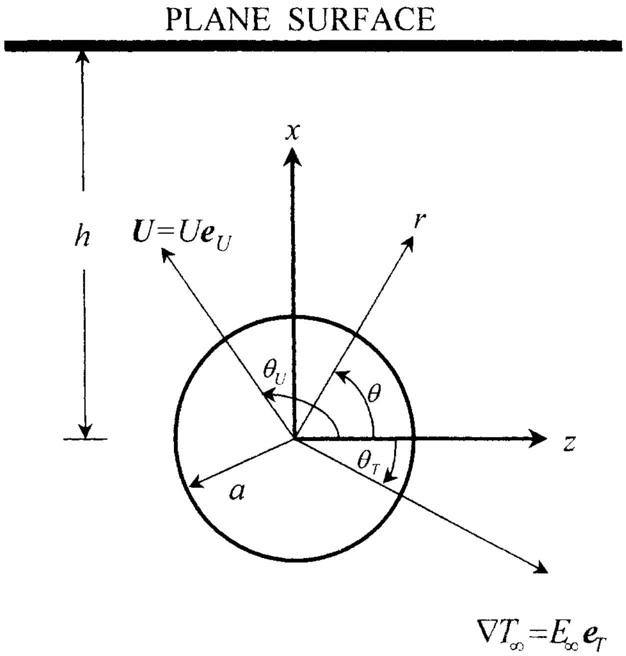

Figure 1. Sphere in the proximity of a plane surface.

Problem Statement

As shown in Figure 1, the thermophoretic motion of a spherical particle of radius a in proximity to an infinite surface at a distance h from the center of the sphere is considered. The plane can be a solid wall (with no-slip boundary) or a free surface (with perfect-slip boundary). A linear temperature field $T_\infty(\boldsymbol{x})$, which is in an arbitrary direction with respect to the plane, with a uniform thermal gradient $E_\infty \boldsymbol{e}_T$ (equal to ∇T_∞) (where $\boldsymbol{e}_T$ is a unit vector in the direction of the temperature gradient) is imposed on the surrounding gaseous medium far away from the sphere. The particle center is chosen to be at the origin of the righthanded Cartesian coordinate system for convenience. In addition to the rectangular coordinates, the spherical coordinate system (r, θ, ϕ) is also employed. The fluid, which is Newtonian and incompressible, is allowed to slip, both thermally and frictionally, and the temperature jump may occur at the particle surface. The gravitational effect and the Brownian motion of the particle are ignored. The purpose here is to determine the correction of Eq. 1 on the particle velocity due to the presence of a solid wall and/or a free surface.

The transport of momentum and energy is inherently unsteady in the present problem of the thermophoresis of a sphere in the vicinity of a plane boundary. However, the problem can be considered quasi steady if the Peclet and the Reynolds numbers are small (that is, the effects of convection are neglected). The energy equation governing the temperature distribution $T(\boldsymbol{x})$ for the fluid phase of constant conductivity k is the Laplace's equation

$$\nabla^2 T = 0. \tag{2a}$$

For the particle we have

$$\nabla^2 T_i = 0, \tag{2b}$$

where $T_i(\boldsymbol{x})$ is the temperature field inside the particle. The boundary condition at the particle surface requires that the normal heat fluxes be continuous and a temperature jump that is proportional to the normal temperature gradient (Kennard, 1938) must occur. The fluid temperature must approach the prescribed linear field far away from the particle, and the temperature inside the particle is finite everywhere. Thus, we have

$$r = a \qquad k\nabla T \cdot \boldsymbol{e}_r = k_i \nabla T_i \cdot \boldsymbol{e}_r, \tag{3a}$$

$$T - T_i = C_t l \nabla T \cdot \boldsymbol{e}_r, \tag{3b}$$

$$r < a \qquad T_i \ \text{is finite}, \tag{3c}$$

$$x = h \qquad T = T_\infty \cos\theta_T, \tag{3d}$$

$$x \le h,\ y^2 + z^2 \to \infty \qquad \nabla T \to \nabla T_\infty, \tag{3e}$$

where $\boldsymbol{e}$ is the radial unit vector in the spherical coordinates; $\cos\theta_T = \boldsymbol{e}_T \cdot \boldsymbol{e}_z$, with $\boldsymbol{e}_z$ being the unit vector of the z-component in the rectangular coordinates; and k_i is the thermal conductivity of the particle, which is assumed to be independent of temperature. In Eq. 3b, l is the mean free path of the surrounding fluid, and C_t refers to the dimensionless temperature jump coefficient at the particle surface.

Since the low Reynolds number is encountered in the thermophoretic motion, the velocity field $\boldsymbol{v}$ and the dynamic pressure field p satisfy the Stokes equations

$$\eta \nabla^2 \boldsymbol{v} - \nabla p = \boldsymbol{0}, \tag{4a}$$

$$\nabla \cdot \boldsymbol{v} = 0. \tag{4b}$$

Owing to the thermal creep velocity and the frictional slip velocity along the particle surface as well as the fluid at rest far away from the particle, the boundary conditions for the fluid flow field are

$$r = a \qquad \boldsymbol{v} = \boldsymbol{U} + a\boldsymbol{\Omega} \times \boldsymbol{e}_r + \frac{C_m l}{\eta}(\boldsymbol{I} - \boldsymbol{e}_r\boldsymbol{e}_r)\boldsymbol{e}_r : \boldsymbol{\tau}$$

$$+ C_s \frac{\eta}{\rho T_0}(\boldsymbol{I} - \boldsymbol{e}_r\boldsymbol{e}_r) \cdot \nabla T, \tag{5a}$$

$$\boldsymbol{v} = \boldsymbol{0} \qquad \text{(for the solid wall situation)}$$

$$x = h \quad \left.\begin{aligned} &\boldsymbol{e}_x \cdot \boldsymbol{v} = 0 \\ &(\boldsymbol{I} - \boldsymbol{e}_x\boldsymbol{e}_x)\boldsymbol{e}_x : \boldsymbol{\tau} = \boldsymbol{0} \end{aligned}\right\} \text{(for the free surface sitaution)}, \tag{5b}$$

$$x \le h,\ y^2 + z^2 \to \infty \qquad \boldsymbol{v} \to \boldsymbol{0}. \tag{5c}$$

Here, T_0 is the prescribed temperature at the particle center; $\boldsymbol{\tau}(= \eta[\nabla \boldsymbol{v} + (\nabla \boldsymbol{v})^T])$ is the viscous stress tensor for the fluid; $\boldsymbol{e}_x$ is the unit vector of the x-component in the rectangular coordinates; C_m and C_s are the dimensionless hydrodynamic slip and thermal slip coefficients, respectively, at the particle surface; and $\boldsymbol{U}$ and $\boldsymbol{\Omega}$ are the instantaneous translational and angular velocities, respectively, of the aerosol sphere to be determined. Two situations in the boundary conditions at the plane surface are described in Eq. 5b. One is that the fluid velocity disappears if the plane is a solid wall, which is the most popular boundary condition described at a solid–fluid interface. The other boundary condition at the plane is that the normal component of fluid velocity and the tangential shear stress of the fluid disappear, which means that the plane is a gas–liquid free surface (or, say, a perfect slip boundary). Note also that the interfacial tension is assumed to be large enough to maintain the planarity of the free surface.

Since the particle is freely suspended in the surrounding fluid, the temperature field produces no net force and torque on the particle. Thus, to determine the particle velocity, the requirement of zero force and torque exerted by the fluid on the particle surface should be satisfied.

Analysis

For the motion of a freely suspended sphere under an arbitrary applied temperature field $T_A(\boldsymbol{x})$ and a velocity field $\boldsymbol{v}_A(\boldsymbol{x})$ in an unbounded fluid, the translational and the angular velocity of the particle can be obtained by combining the general Brock's equation (Keh and Chen, 1995) and the modified Faxen's law for a sphere with slip boundary (Keh and Chen, 1996b):

$$\boldsymbol{U} = A(\nabla T_A)_0 + (\boldsymbol{v}_A)_0 + \frac{1}{6}a^2 D(\nabla^2 \boldsymbol{v}_A)_0, \tag{6a}$$

$$\boldsymbol{\Omega} = \frac{1}{2}(\nabla \times \boldsymbol{v}_A)_0, \tag{6b}$$

where a is the particle radius; the subscript 0 denotes the position of the sphere center; while the coefficients A and D are defined as

$$A = -2C_s \frac{\eta}{\rho (T_A)_0}\left[\frac{1 + k^* C_t^*}{(1 + 2C_m^*)(2 + k^* + 2k^* C_t^*)}\right], \tag{7a}$$

$$D = \frac{1}{1 + 2C_m^*}. \tag{7b}$$

In Eq. 7b, $k^* = k_i/k$ is the ratio of thermal conductivity between the particle and the surrounding fluid; $C_m^* = C_m l/a$; and $C_t^* = C_t l/a$. The superposition of the thermophoretic and the hydrodynamic contributions in Eq. 6 is valid due to the linearity of the governing equations and the boundary conditions in the problem.

In situation $a/h \ll 1$, a method of reflections (Happel and Brenner, 1983; Chen and Keh, 1990; Chen, 1999, 2000) is used to solve the motion of a sphere in the vicinity of a plane surface. The solution of local temperature and velocity fields for the fluid surrounding the aerosol particle can be decomposed into a sum of fields, which depends on the increasing power of $\lambda (= a/h$; the ratio of the sphere radius to the distance of the sphere center from the plane boundary),

$$T = T_\infty + T_p^{(1)} + T_w^{(1)} + T_p^{(2)} + T_w^{(2)} + \dots, \tag{8a}$$

$$v = v_p^{(1)} + v_w^{(1)} + v_p^{(2)} + v_w^{(2)} + \dots, \tag{8b}$$

where the subscripts p and w represent the reflections from the particle and the plane surface, respectively, and the superscript (i) denotes the ith reflection from that surface. In these series, all the sets of the corresponding temperature fields and velocities must satisfy Eqs. 2a and 4. The advantage of this method is that the boundary-value problem can be solved to any degree of approximation by considering the boundary conditions associated with only one surface at a time.

According to Eq. 8, the particle velocity can also be expressed in the form of the series

$$U = U^{(0)} + U^{(1)} + U^{(2)} \dots, \tag{9a}$$

$$\Omega = \Omega^{(0)} + \Omega^{(1)} + \Omega^{(2)} \dots, \tag{9b}$$

where $U^{(i)}$ and $\Omega^{(i)}$ are related to $T_w^{(i)}$ and $v_w^{(i)}$ by Eq. 6.

While inspecting the linearity of the problem, one can decompose the thermophoretic motion of a sphere in the proximity of a plane into two independent problems: (1) the thermophoretic motion of a sphere perpendicular to a plane boundary, and (2) the thermophoretic motion of a sphere parallel to a plane boundary. In these two cases, the choice of the y- and z-directions in the yz plane is arbitrary. Therefore, it is convenient to choose the later problem for the motion parallel to the surface such that the thermal gradient points in just one of the coordinate directions, chosen here as the z-direction. Thus, the translational and rotational velocities of a particle driven by an arbitrary prescribed temperature gradient with respect to the plane surface can be expressed as

$$U = \left[M^{(n)} e_x e_x + M^{(p)} (I - e_x e_x) \right] \cdot U^{(0)}, \tag{10a}$$

$$a\Omega = -N e_x \times U^{(0)}, \tag{10b}$$

where $M^{(n)}$, $M^{(p)}$, and N are the dimensionless mobility functions, and $U^{(0)}$ is computed from Eq. 1. In the following two subsections, we deal with the axisymmetric motion of a thermophoretic sphere normal to a plane, and the asymmetric motion of a particle parallel to a plane. In the first situation, the temperature gradient is aligned perpendicular to the plane surface ($\nabla T_\infty = E_\infty e_x$), while in the second, the gradient is parallel to the plane ($\nabla T_\infty = E_\infty e_z$).

Thermophoretic motion normal to a plane

In this case, the motion caused by the temperature gradient is normal to the plane boundary, and the temperature and flow fields are axially symmetric. Owing to the low Reynolds number encountered in the thermophoretic motion, the fluid flow is governed by the quasi-steady fourth-order differential equation of stream function for viscous axisymmetric flow. The stream function satisfies the Stokes equations, while the temperature distributions, inside and outside the particle, satisfy Laplace's equation. This problem was formulated analytically by using a method of reflections (Chen, 1999), and therefore much of the detail is omitted here.

The final expressions for the translational mobility function of the particle immersed in the axisymmetric flow field are

$$M_s^{(n)} = 1 - \frac{1}{4}(G+2)\lambda^3 + \frac{1}{4}D\lambda^5 + \frac{1}{256}\left(32G + 16G^2 - 135C_1 + 108\frac{B}{A}G\right)\lambda^6 + \frac{1}{512}\left(32DG - 180\frac{B}{A}G - 150GH + 135C_1 D - 108\frac{B}{A}DG\right)\lambda^8 + O(\lambda^9), \tag{11a}$$

for the thermophoretic motion normal to a solid wall, and

$$M_f^{(n)} = 1 - \frac{1}{8}(2G+1)\lambda^3 + \frac{1}{128}\left(4G + 8G^2 - 15C_1 + 36\frac{B}{A}G\right)\lambda^6 - \frac{3}{512}\left(12\frac{B}{A}G + 50GH - 5C_1 D + 12\frac{B}{A}DG\right)\lambda^8 + O(\lambda^9), \tag{11b}$$

for the movement toward a free surface. In Eq. 11, coefficients A and D are defined in Eq. 7, whereas, B, C_1, G, and H are defined as

$$B = \frac{5}{2}C_s \frac{\eta}{\rho T_0}\left[\frac{1 + 2k^* C_t^*}{(1+5C_m^*)(3 + 2k^* + 6k^* C_t^*)}\right], \tag{12a}$$

$$C_1 = \frac{1 + 2C_m^*}{1 + 5C_m^*}, \tag{12b}$$

$$G = \frac{1 - k^* + k^* C_t^*}{2 + k^* + 2k^* C_t^*}, \tag{12c}$$

$$H = \frac{1 - k^* + 2k^* C_t^*}{3 + 2k^* + 6k^* C_t^*}. \tag{12d}$$

The $O(\lambda^9)$ interactions in Eq. 11 are neglected, but the numerical significance would be small unless the gap between the surfaces of the particle and the plane approaches zero. Note that, the mobility functions, $M_s^{(n)}$ and $M_f^{(n)}$, in Eq. 11 are independent of the thermal slip coefficient C_s. Moreover, the rotational mobility function (N) will vanish in this case, since the flow field around the particle is axially symmetric.

Thermophoretic motion parallel to a plane

In this subsection, the asymmetric motion of a thermophoretic sphere parallel to a solid wall (no-slip) and/or a free surface (perfect-slip) is considered. This problem has not been addressed in the past studies. Here, the prescribed temperature gradient is $\nabla T_\infty = E_\infty \mathbf{e}_z$. A method of reflections is used to solve this problem. For conciseness, detailed derivations in the temperature and velocity fields and their corresponding particle velocities are formulated in the Appendix. A comparison between Eqs. 10 and A12 gives

$$M_s^{(p)} = 1 - \frac{1}{8}(1+G)\lambda^3 + \frac{3}{32}D\lambda^5 + \frac{1}{256}\left(4G + 4G^2 + 36\frac{B}{A}G - 45C_1\right)\lambda^6 + \frac{3}{2{,}048}\left(16GH - 48\frac{B}{A}G - 8DG - 44\frac{B}{A}DG + 55C_1 D + 3C_2 D + 36C_3\right)\lambda^8 + O(\lambda^9), \quad (13a)$$

$$N_s = -\frac{3}{64}\lambda^4 + \frac{3}{1{,}024}\left(8G + 384\frac{B}{A}G - 30C_1 - 5C_2\right)\lambda^7 - \frac{3}{128}\left(4\frac{B}{A}G - 3C_3\right)\lambda^9 + O(\lambda^{10}), \quad (13b)$$

for the thermophoretic motion parallel to a solid wall, and

$$M_f^{(p)} = 1 - \frac{1}{16}(1+2G)\lambda^3 + 0\lambda^5 + \frac{1}{128}(G+2G^2)\lambda^6 + \frac{1}{1{,}024}\left(24GH + 24\frac{B}{A}G - 24\frac{B}{A}DG + 10C_1 D - 9C_3\right)\lambda^8 + O(\lambda^9), \quad (13c)$$

$$N_f = \frac{3}{512}\left(12\frac{B}{A}G - 5C_1\right)\lambda^7 + O(\lambda^{10}), \quad (13d)$$

for the movement nearby a free surface. In Eq. 13, the $O(\lambda^9)$ and $O(\lambda^{10})$ interactions of the translational and rotational mobilities are ignored, respectively, and the coefficients C_2 and C_3 are defined as

$$C_2 = \frac{1}{1+3C_m^*}, \quad (14a)$$

$$C_3 = \frac{1}{1+5C_m^*}. \quad (14b)$$

Similar to the axisymmetric case, the mobility functions $M_s^{(p)}$, $M_f^{(p)}$, N_s, and N_f in Eq. 13 are independent of the thermal slip coefficient C_s. It should be noted that the contribution of k^* and C_t^* to the boundary effect on the translational mobility is of $O(\lambda^3)$, while the contribution of C_m^* is of $O(\lambda^5)$ for a solid wall situation or $O(\lambda^8)$ for a free surface situation. On the other hand, the contribution of k^*, C_t^*, and C_m^* to the boundary effect on the rotational mobility is of $O(\lambda^7)$.

There are some limitations resulting from Eq. 13. First, when there is no temperature jump ($C_t^* = 0$) and no hydrodynamic slip velocity ($C_m^* = 0$) at the particle–fluid interface, then the thermophoretic velocity in Eq. 13 can be reduced as

$$M_s^{(p)} = 1 - \frac{3}{8(2+k^*)}\lambda^3 + \frac{3}{32}\lambda^5 - \frac{3(236 + 304k^* + 128k^{*2} + 15k^{*3})}{256(2+k^*)^2(3+2k^*)}\lambda^6 + \frac{9(262 + 173k^* + 35k^{*2})}{2{,}048(2+k^*)(3+2k^*)}\lambda^8 + O(\lambda^9), \quad (15a)$$

$$N_s = -\frac{3}{64}\lambda^4 - \frac{3(1{,}146 - 227k^* - 394k^{*2})}{1{,}024(2+k^*)(3+2k^*)}\lambda^7 + \frac{3(14+k^*)}{128(3+2k^*)}\lambda^9 + O(\lambda^{10}), \quad (15b)$$

$$M_f^{(p)} = 1 - \frac{4-k^*}{16(2+k^*)}\lambda^3 + \frac{(1-k^*)(4-k^*)}{128(2+k^*)^2}\lambda^6 + \frac{30 - 41k^* + 26k^{*2}}{1{,}024(2+k^*)(3+2k^*)}\lambda^8 + O(\lambda^9), \quad (15c)$$

$$N_f = -\frac{15(6-k^*)}{512(3+2k^*)}\lambda^7 + O(\lambda^{10}). \quad (15d)$$

On the other hand, by considering the influence of k^* on the thermophoretic velocity, we may get

$$M_s^{(p)} = 1 - \frac{3}{16}\lambda^3 + \frac{3}{32(1+2C_m^*)}\lambda^5 - \frac{3(19+35C_m^*)}{256(1+5C_m^*)}\lambda^6 + \frac{393 + 2{,}089C_m^* + 2{,}996C_m^{*2} + 960C_m^{*3}}{2{,}048(1+2C_m^*)(1+3C_m^*)(1+5C_m^*)}\lambda^8 + O(\lambda^9), \quad (16a)$$

$$N_s = -\frac{3}{64}\lambda^4 - \frac{3(191 + 943C_m^* + 1{,}080C_m^{*2})}{1{,}024(1+3C_m^*)(1+5C_m^*)}\lambda^7 + \frac{7+5C_m^*}{64(1+5C_m^*)}\lambda^9 + O(\lambda^{10}), \quad (16b)$$

$$M_f^{(p)} = 1 - \frac{1}{8}\lambda^3 + \frac{1}{128}\lambda^6 + \frac{5}{1{,}024(1+5C_m^*)}\lambda^8 + O(\lambda^9), \quad (16c)$$

$$N_f = -\frac{15(1+2C_m^*)}{256(1+5C_m^*)}\lambda^7 + O(\lambda^{10}), \quad (16d)$$

for a thermally insulated sphere ($k^* \to 0$), and

$$M_s^{(p)} = 1 - \frac{3C_t^*}{8(1+2C_t^*)}\lambda^3 + \frac{3}{32(1+2C_m^*)}\lambda^5 - \frac{3}{64}\left[\frac{C_t^*(1-C_t^*)}{(1+2C_t^*)^2} + \frac{15(1+2C_m^*)C_t^*}{(1+5C_m^*)(1+3C_t^*)}\right]\lambda^6 + \frac{3}{2{,}048}\left[\frac{91}{1+5C_m^*} + \frac{3}{(1+2C_m^*)(1+3C_m^*)} + \frac{8(1-C_t^*)}{(1+2C_m^*)(1+2C_t^*)} - \frac{5(23+24C_m^*)(1-C_t^*)}{(1+5C_m^*)(1+3C_t^*)} + 8\frac{(1-C_t^*)(1-2C_t^*)}{(1+2C_t^*)(1+3C_t^*)}\right]\lambda^8 + O(\lambda^9), \quad (17a)$$

$$N_s = -\frac{3}{64}\lambda^4 - \frac{3}{1{,}024}\left[\frac{5}{1+3C_m^*} + \frac{8(1-C_t^*)}{1+2C_t^*} - \frac{30(1+2C_m^*)(15-19C_t^*)}{(1+5C_m^*)(1+3C_t^*)}\right]\lambda^7 + \frac{3}{128}\left[\frac{3}{1+5C_m^*} - \frac{5(1+2C_m^*)(1-C_t^*)}{(1+5C_m^*)(1+3C_t^*)}\right]\lambda^9 + O(\lambda^{10}), \quad (17b)$$

$$M_f^{(p)} = 1 + \frac{1-4C_t^*}{16(1+2C_t^*)}\lambda^3 + \frac{(1-C_t^*)(1-4C_t^*)}{128(1+2C_t^*)^2}\lambda^6 + \frac{1}{1{,}024}\left[\frac{1}{1+5C_m^*} + 60\frac{C_m^*(1-C_t^*)}{(1+5C_m^*)(1+3C_t^*)} + 12\frac{(1-C_t^*)(1-2C_t^*)}{(1+2C_t^*)(1+3C_t^*)}\right]\lambda^8 + O(\lambda^9), \quad (17c)$$

$$N_f = \frac{15(1+2C_m^*)(1-3C_t^*)}{256(1+5C_m^*)(1+3C_t^*)}\lambda^7 + O(\lambda^{10}), \quad (17d)$$

for a well-conductive particle ($k^* \to \infty$). Note that the thermophoretic velocity of an aerosol sphere parallel to a plane surface will disappear in the limited situation where $C_m^* \to \infty$ (since $U^{(0)} = \mathbf{0}$), although the values of thermophoretic mobilities $M_s^{(p)}$, $M_f^{(p)}$, N_s, and N_f may be finite.

Results and Discussion

The interaction between an aerosol sphere and a plane boundary in a temperature gradient field, given by Eqs. 10, 11, and 13, results from three phenomena. First, the presence of a boundary disturbs the local temperature field experienced by the particle, which causes the thermophoretic behavior of the particle to deviate from its behavior when it is isolated. Second, the boundary drags the surrounding fluid (hydrodynamic slip at the particle surface is allowed though) that convects and rotates the particle. Third, the boundary characteristic (no-slip or perfect slip) affects the thermal creep effect that occurs at the surface of the particle, which in turn influence the motion of the particle. Since both the temperature gradient and the velocity disturbances in the fluid phase produced by an isolated thermophoretic sphere decay according to r^{-3} (where r is the distance from the particle center) (Keh and Chen, 1995), as shown in Eqs. 11 and 13, the leading term of the interaction for particle translation is $O(\lambda^3)$ ($\lambda = a/h$; the ratio of the sphere radius to the distance of the sphere center from the planar wall). For a thermophoretic sphere that allows free rotation, the leading term of the angular velocity is $O(\lambda^4)$ for a solid-wall situation or $O(\lambda^7)$ for a free-surface situation. Thus, the interaction between a particle and a plane surface undergoing thermophoresis is much weaker than that between a sedimenting particle and a plane, since the leading terms of a particle in motion for translational and angular velocities of a sphere in the vicinity of a plane wall by the body force are $O(\lambda)$ and $O(\lambda^2)$, respectively (Keh and Chen, 1997). In sedimentation, there is a net gravitational force exerted on the particle, and this force is balanced by a nonzero hydrodynamic force. However, there is no hydrodynamic force exerted on the particle in thermophoretic motion. As a comparison, the disturbance velocity fields in the surrounding fluid for the two situations decay at a different rate with λ.

Thermophoresis of a sphere normal to a plane

When the prescribed temperature gradient is in the direction normal to the plane boundary, the problem was formulated in our previous study (Chen, 1999), where not only the particle velocity but also the thickness of the thermophoretic interacting region and the deposition time for a particle translating perpendicularly through the interacting region were presented. Several important conclusions resulted from this investigation of axisymmetric thermophoresis. First, the interaction effects between the particle and the boundary on the thermophoretic motion are in general much weaker than those on sedimentation, since the disturbance to the fluid velocity caused by a thermophoretic sphere decays faster (as r^{-3}) (Keh and Chen, 1995) than that caused by a settling particle (as r^{-1}) (Keh and Chen, 1996b). Second, the thermophoretic velocity for an aerosol sphere perpendicular to a solid wall is always smaller than the velocity it would possess if isolated. If the plane boundary is a free surface, however, the particle velocity may be either greater or smaller than the velocity when there is no plane in the vicinity. For all specified cases, a solid wall where the velocity must vanish produces a greater effect on the particle motion than does a free surface where only the normal component of the velocity vanishes. Third, a particle with large thermal conductivity will translate faster than the one whose thermal conductivity is relatively small under the influence of the plane. Fourth, the influence of interactions between the particle and the plane on the axisymmetric thermophoretic velocity is more significant as the value of the internal-to-external conductivity ratio of the particle (k^*) becomes smaller. Fifth, the thickness of the thermophoretic interacting region affecting a sphere translating normally to a solid wall will decrease monotonically when the k^* is increasing or C_t^* and C_m^* are decreasing. However, the thickness of the interacting region for a particle migrating perpendicular to a free surface is not a monotonically decreasing function of k^* if the values of C_t^* and C_m^* are small.

Thermophoresis of a sphere parallel to a plane

Here we consider the asymmetric thermophoresis of a sphere parallel to a plane where a linear temperature profile is prescribed. The thermophoretic mobilities of translation and rotation for various cases of a spherical particle, wherein the surrounding fluid may slip thermally and hydrodynamically at the particle–fluid interface, moving parallel to a solid wall and/or a free surface, are shown in Figures 2–5. As expected, the results illustrate that the boundary effect decreases rapidly, for all values of k^*, C_t^*, and C_m^*, with decreasing λ. However, the interaction between the boundary and the particle gets significant when the gap between the particle surface and the plane decreases. In addition, for all specified values of k^*, C_t^*, and C_m^*, the solid surface where the velocity must vanish produces a greater effect on the particle motion than does the free surface, where only the normal component of the velocity vanishes.

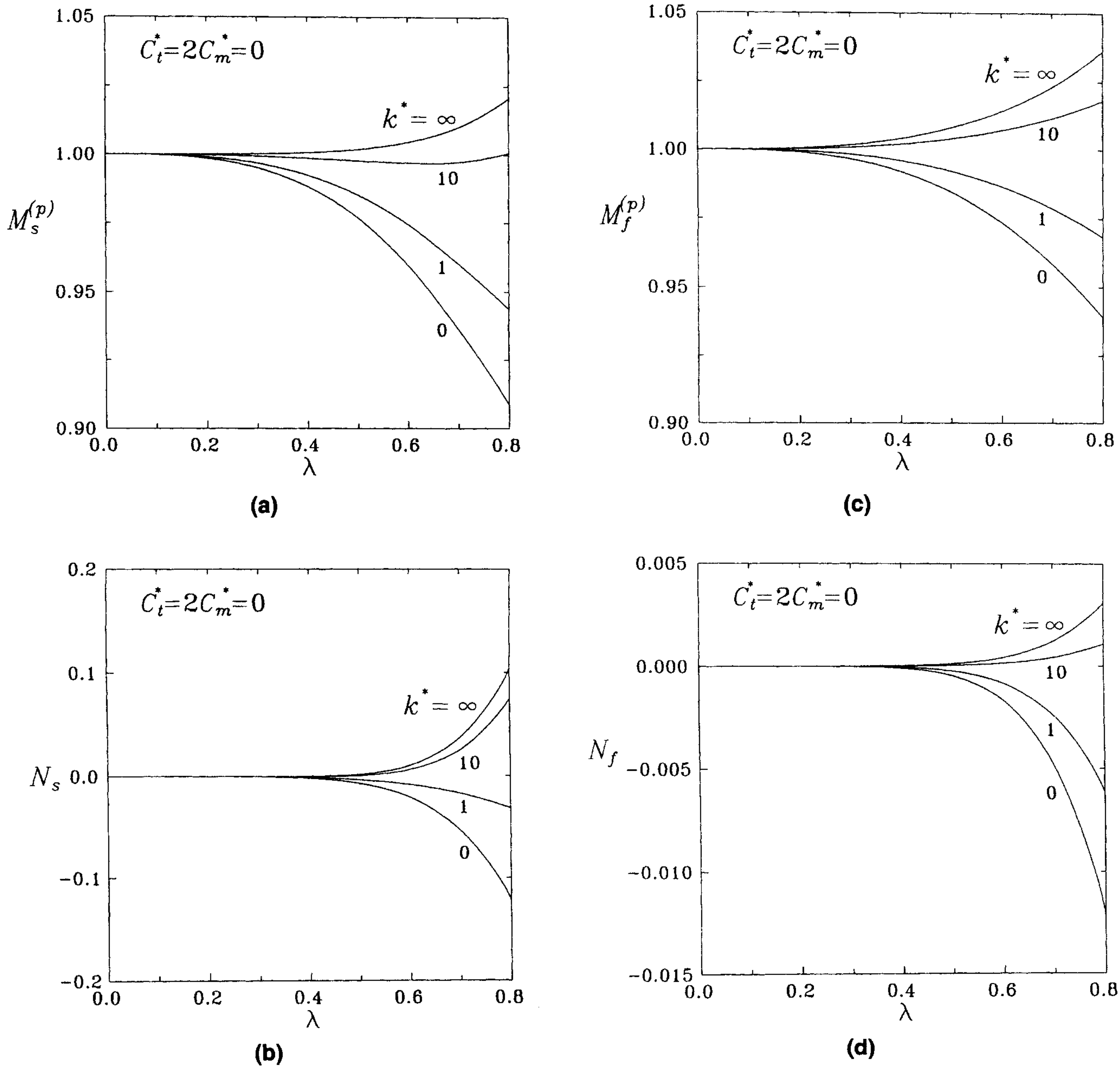

Figure 2. Translational and rotational mobilities of a sphere parallel to a conductive plane vs. separation parameter λ with k^* as a parameter ($C_t^* = 0$, $C_m^* = 0$): (a), (b) solid wall plane; (c), (d) free surface plane.

In Figures 2, 3 and 4, the translating and the rotating mobilities of a particle are plotted against the separation parameter λ with k^* as a parameter. The figures show that the translational velocity of a thermophoretic sphere with a small thermal conductivity moving parallel to a plane (either a solid wall or a free surface) is less than the velocity that the sphere would possess if isolated, that is, the motion of a less conductive particle will move slowly as it approaches the boundary. This retardation effect on the particle motion is similar to the case when gravity is the driving force for the migration of an aerosol particle (Chen and Keh, 1995b). However, the interaction between the particle and the plane in thermophoresis is much weaker than that in a body-force field. On the contrary, when the particle is relatively conductive, the hindrance effect on the particle motion due to the presence of a plane boundary may become an enhancement factor to the velocity of a thermophoretic sphere. A thermophoretic particle with large conductivity will translate more quickly than it would if isolated. Moreover, this enhancement on the particle motion will be more significant if the plane is a free surface than if the plane were a solid wall. In practical applications, the values of k^* are usually much greater than 1, that is, when an aerosol particle is moving parallel to a plane in the direction of the temperature gradient, the particle will

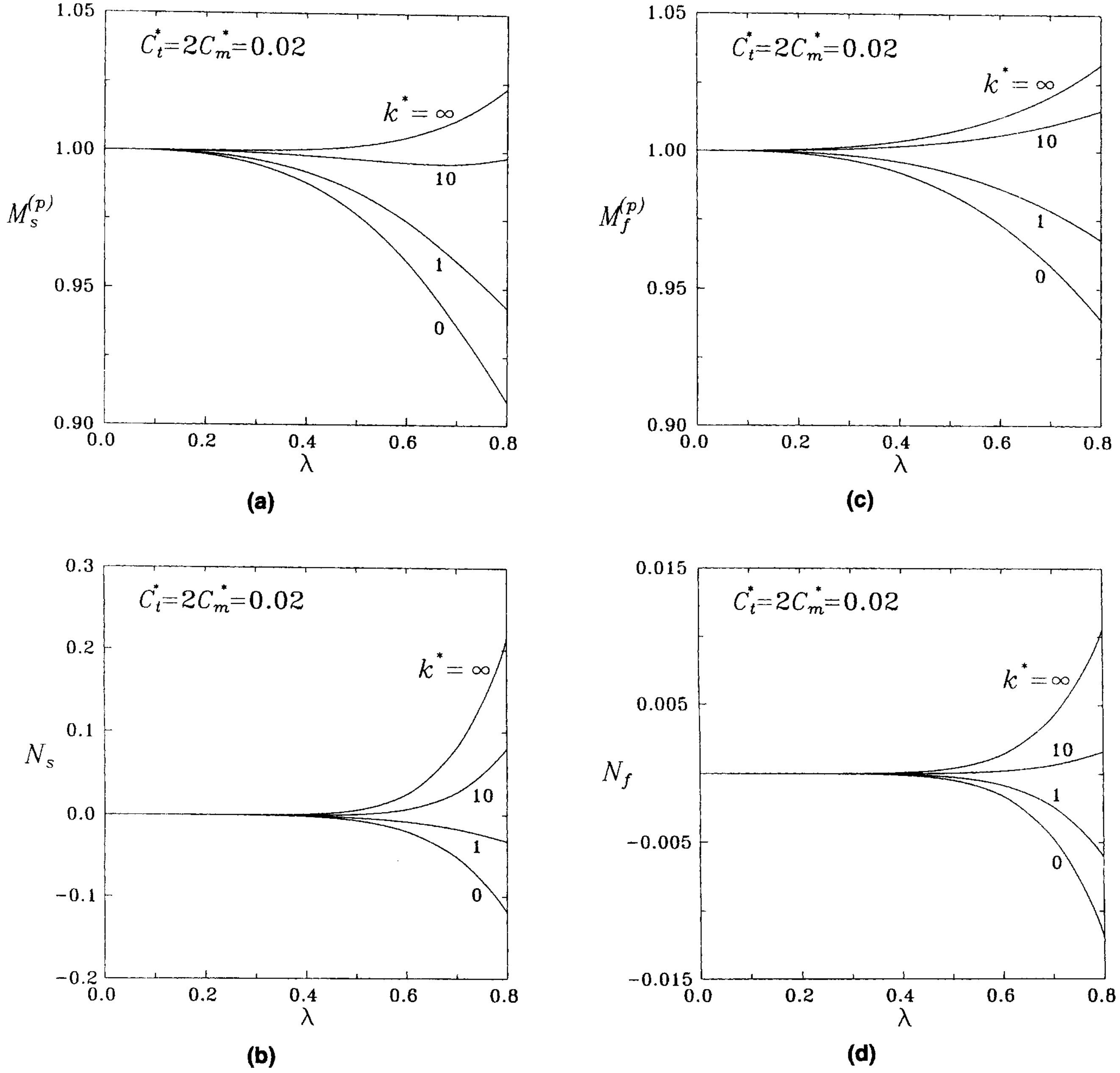

Figure 3. Translational and rotational mobilities of a sphere parallel to a conductive plane vs. separation parameter λ with k^* as a parameter ($C_t^* = 0.02$, $C_m^* = 0.01$): (a), (b) solid wall plane; (c), (d) free surface plane.

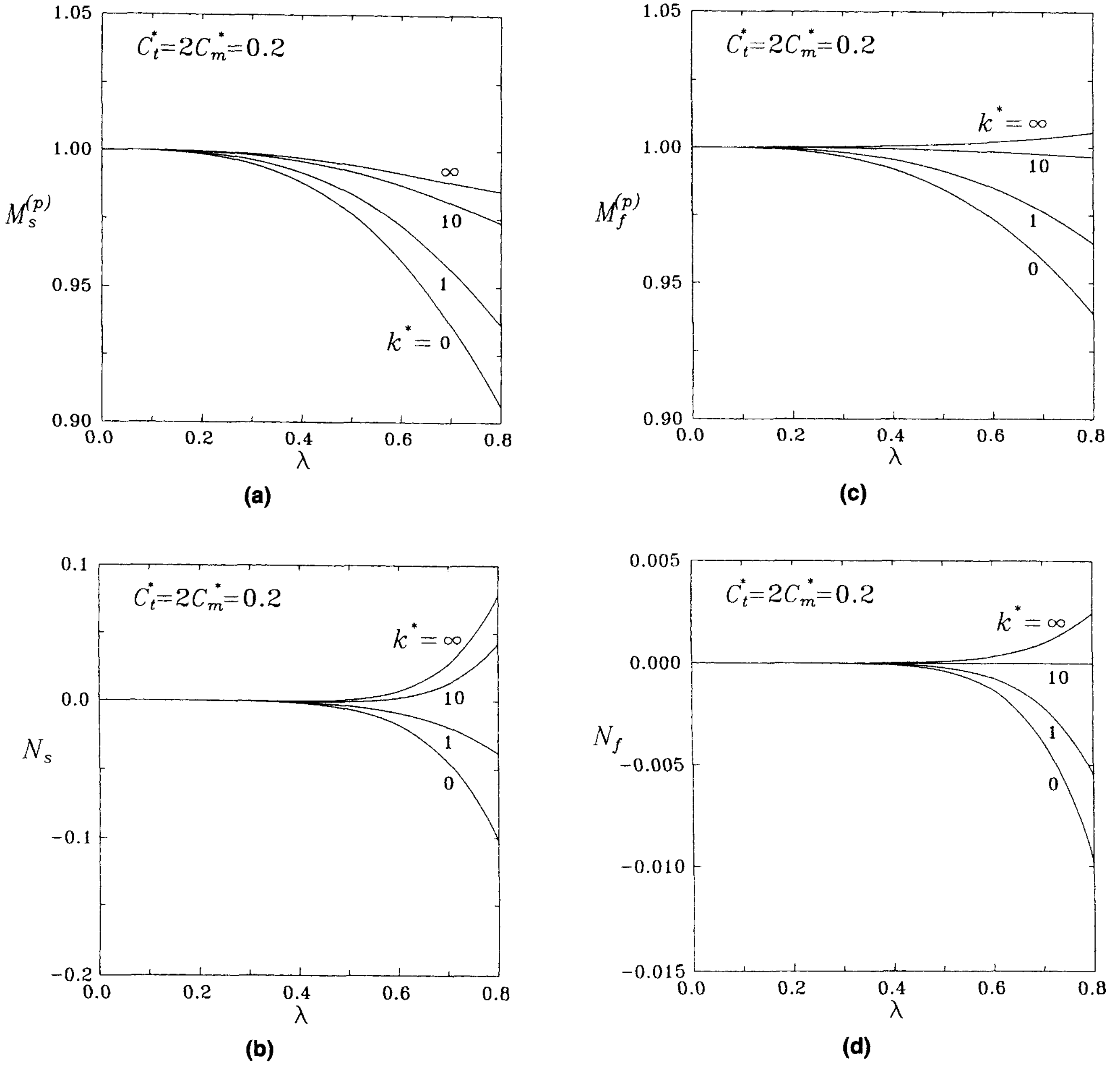

Figure 4. Translational and rotational mobilities of a sphere parallel to a conductive plane vs. separation parameter λ with k^* as a parameter ($C_t^* = 0.2$, $C_m^* = 0.1$): (a), (b) solid wall plane; (c), (d) free surface plane.

translate faster than that if the particle is far away from the plane. This phenomenon is quite different from that of the motion when the particle is translating normally to the solid wall where the wall temperature is kept constant (Chen, 1999), and/or parallel to an adiabatic wall (Chen, 2000). Moreover, for all the specified cases illustrated in Figures 2–4, a particle with a large thermal conductivity will translate faster than one whose thermal conductivity is small under the influence of a plane boundary. This characteristic is the same as the thermophoretic motion when a particle is moving normally to a free surface, but it is the reverse of the movement of a particle parallel to a thermally insulated wall, where a particle with high thermal conductivity will migrate slower than a particle with low conductivity. The translational mobilities shown in Figures 2, 3 and 4 indicate that the influence of the interactions between the particle and the plane on the asymmetric thermophoresis is more significant as the value of k^* becomes smaller. In such a case, the particle migrating velocity will decrease monotonically as the value of k^* decreases for all the specified values of separation parameter λ. When considering the influence of the surface properties C_m^* and C_t^* on the particle motion, the situation is much more complicated; the deviation behavior of the particle from when it is isolated is not a monotonic function of C_m^* and C_t^*. Gener-

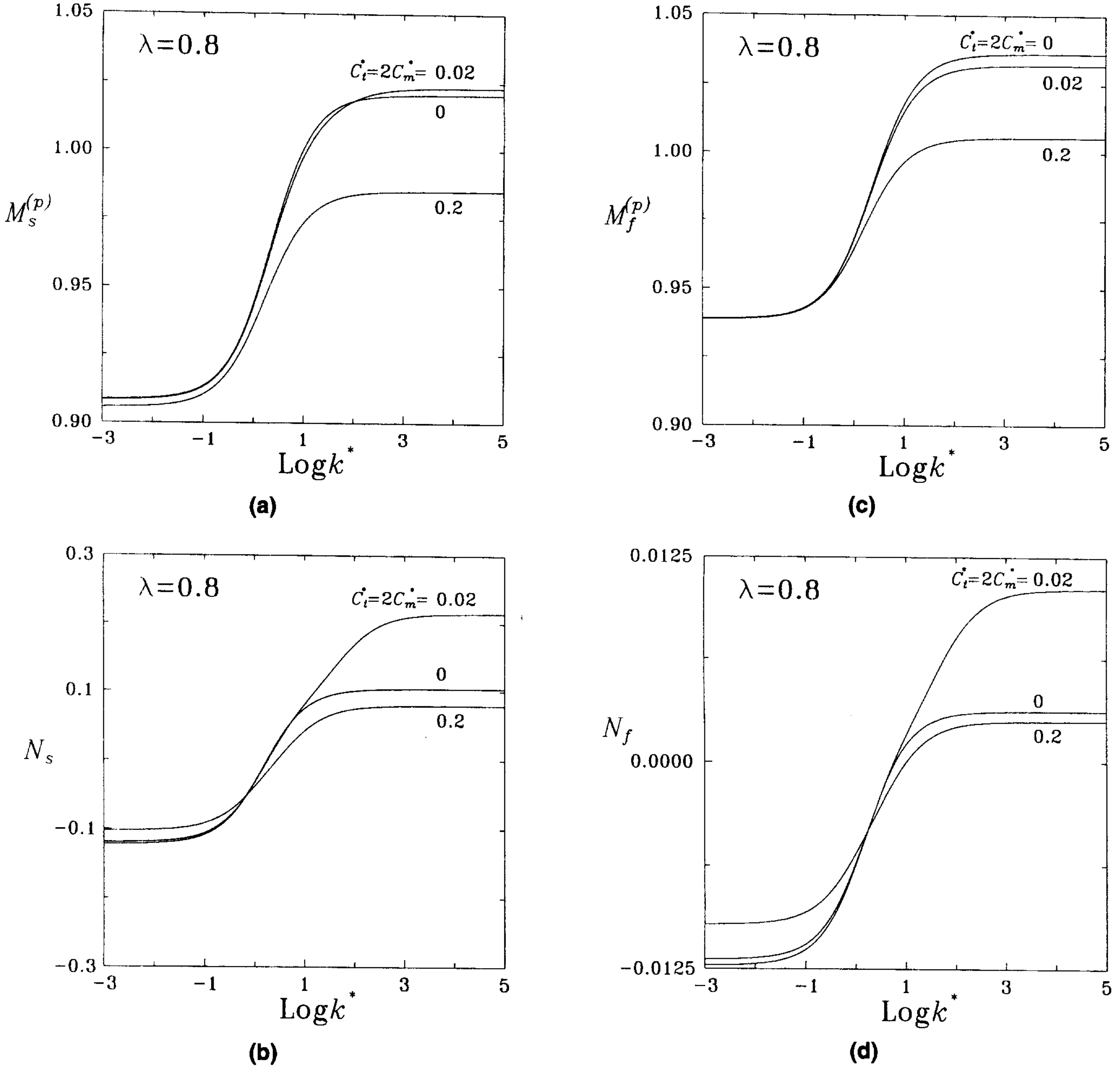

Figure 5. Translational and rotational mobilities of a sphere parallel to a conductive plane vs. conductivity ratio k^* with C_t^* and C_m^* as a parameter ($\lambda = 0.8$): (a), (b) solid wall plane; (c), (d) free surface plane.

ally speaking, the tendencies of the influence of the thermal conductivity ratio (k^*) on the axisymmetric and on the asymmetric motions of a sphere with respect to a thermally conducting plane are consistent with each other. However, these tendencies are in contrast to the motion caused by the asymmetric thermophoresis of a particle parallel to a thermally insulated plane.

On the other hand, both the translational velocity and the rotational velocity will take place due to the asymmetric flow around a particle that is migrating thermophoretically parallel to a plane boundary. The rotational mobility, defined by Eq. 10b, of a thermophoretic sphere parallel to a plane surface is also plotted in Figures 2, 3, and 4. As shown in Figure 1, when a particle is below a surface boundary (either a no-slip wall or a free surface), the direction of the particle rotation is strongly dependent on the value of k^*. Thus, a particle with a small thermal conductivity will rotate clockwise for $E_\infty > 0$, but the rotation will be counterclockwise if the thermal conductivity of a particle is moderate or more. This rotational direction is opposite to the situation where the plane boundary is an adiabatic wall (Chen, 2000); a particle with small thermal conductivity rotates in the counterclockwise direction according to the influence of a thermally insulated plane, while the rotational direction will be clockwise when the relative conductivity of the particle is large. In fact, if one carefully checks the rotational velocity of a well-conductive particle that is moving parallel to a solid wall (as shown in Figures 2b, 3b, and 4b), its rotational direction is not unchangeable as it approaches the wall. In that situation, the particle will first rotate clockwise with an increase in λ, then, as the gap between the surfaces of the particle and the solid wall gets smaller, it will start rotating in a counterclockwise direction. However, the absolute value of the particle rotation when it is clockwise is very small, so it cannot be observed in the figures. In general, the influence of the boundary effect on the angular mobility will be more notable when the plane is a solid wall, and it is not a monotonic function of the surface properties C_m^* and C_t^*. Note that in a specific situation when $C_t^* = 2C_m^* = 0.2$ and $k^* = 10$, the rotational velocity of the thermophoretic sphere parallel to a free surface will vanish, that is, the particle will not be in rotation. This behavior is the same as that of a thermally insulated particle ($k^* = 0$) moving parallel to an adiabatic free surface (Chen, 2000).

In Figure 5, the translational and the rotational mobilities for the thermophoresis of a particle parallel to a thermally conductive plane surface (either a solid wall or a free surface) are plotted vs. k^* with C_m^* and C_t^* as parameters for the case of $\lambda = 0.8$ (that is, the gap between the surfaces of the particle and the plane is one-fourth of the particle radius). It can be seen that the translational and the rotational mobilities of the particle increase monotonically as k^* increases. Also, the translational velocity for the axisymmetric thermophoretic motion of a particle moving normal to a conductive plane will increase with the increase of k^*. However, this tendency will be quite different for the asymmetric thermophoresis of a particle migrating parallel to an insulated plane; there the translational and the rotational mobilities decrease with the increase of k^*. Again, the presence of a plane boundary will retard the movement of a particle with a small k^* value at a specified gap between the particle and the plane ($\lambda = 0.8$), and this influence is remarkable as $k^* \to 0$. When the plane is a free surface, as illustrated in Figure 5c, the retardation effect of a plane boundary on the particle motion is less significant. Moreover, the boundary effect of a plane surface may enhance the translational velocity of a particle with a large thermal conductivity value, and this enhancement effect will be remarkable if the plane close to the thermophoretic particle is a free surface.

In practical applications of thermophoresis, one may wonder how close the surfaces between the particle and the boundary need to be in order to influence the thermophoretic behavior of a particle parallel to the plane boundary. A definition of the thickness of the thermophoretic interacting region, δ, is taken as the distance of the particle center from the plane surface when the particle translating velocity reaches 99% of the value if the particle prevails away from the plane wall. In Figure 6, the thickness of the interacting region that is normalized by the particle radius is plotted against the ratio of thermal conductivity with C_t^* and C_m^* as the parameters. This shows that when k^* increases and C_t^* and C_m^* are small, the thickness of the interacting region will first decrease monotonically to a minimum value, after which the region thickness will instead increase with the increase of k^*. When the plane boundary is a free surface, this minimum value is equal to one ($\delta/a = 1$), which means that the thermophoretic motion of a particle parallel to a conductive free surface will not be influenced by the presence of the boundary under certain specific physical properties (k^*, C_t^*, and C_m^*). This is different from the results due to the thermophoretic motion parallel to a thermally insulated wall, where the thickness of the thermophoretic boundary layer increases monotonically with the increase of k^*. Note that, when the thermal conductivity of the particle is small ($k^* < 0.01$), the thickness of the normalized interacting region is independent of the particle surface

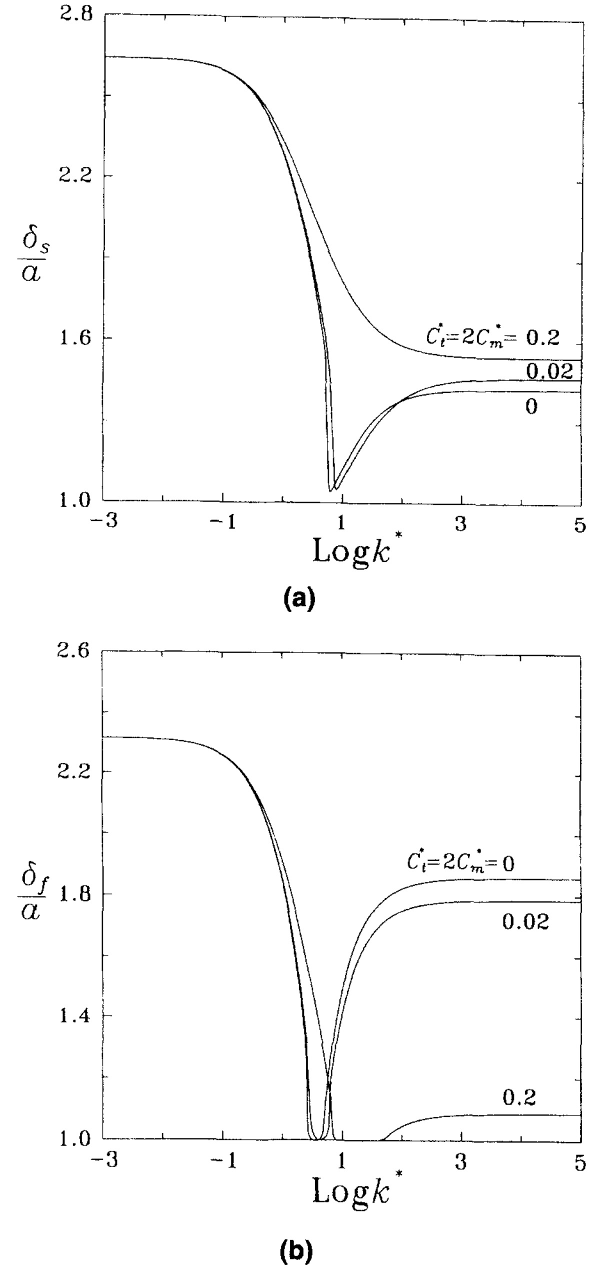

Figure 6. Normalized thickness of the thermophoretic interacting region vs. conductivity ratio k^* with C_t^* and C_m^* as parameters: (a) solid wall plane; (b) free surface plane.

properties, C_t^* and C_m^*. In this case, there is a limited value of $\delta_s/a = 2.64$ for a solid-wall situation or $\delta_f/a = 2.32$ for a free-surface problem. As a comparison between the particle motion normal and parallel to a plane surface, the influence of the boundary effect on the asymmetric thermophoretic motion (particle moving parallel to the plane) is less significant than that on the axisymmetric one (particle moving normal to the plane). That is, the thickness of the interacting region is larger when the particle motion is normal to the plane than when the particle is moving parallel to the boundary. In the case of particle with a small value of thermal conductivity, the region thickness of the thermophoresis for a particle parallel to a solid wall is larger than that when the plane is a free surface, that is, the boundary effect of a solid wall on the particle motion is more remarkable than the effect caused by a free surface. However, this is not true when the thermal conductivity of the particle is large. Then the thickness of the interacting region strongly depends on the surface properties (C_t^* and C_m^*) of the particle.

Thermophoresis in an arbitrary direction

As shown in Figure 1, when the prescribed temperature gradient and the corresponding thermophoretic velocity are $\nabla T_\infty = E_\infty \boldsymbol{e}_T$ (with $\boldsymbol{e}_T \cdot \boldsymbol{e}_z = \cos\theta_T$) and $\boldsymbol{U} = U\boldsymbol{e}_U$ (with $\boldsymbol{e}_U \cdot \boldsymbol{e}_z = \cos\theta_U$), respectively, the translational and the rotational mobilities of a thermophoretic particle are evaluated in Tables 1 and 2 with (θ_T, λ) and (k^*, θ_T) as the parameters, respectively. In general, the specified situations listed in Table 1 show that the presence of a solid wall retards the motion of a thermophoretic sphere ($M_s < 1$) with $k^* = 100$. But it does not continue if the applied temperature gradient is almost parallel to the wall ($\theta_T \approx 0$). On the contrary, this boundary influence on the particle motion can convert into an enhancement factor for a free-surface situation ($M_f > 1$). Both the hindrance effect of the solid wall and the acceleration effect of the free surface on the particle motion are intensified as the gap between the surfaces of the particle and the plane becomes small. That is, due to the direction of the temperature gradient specified in Table 1, the thermophoretic particle will translate slowly as it approaches a solid wall; however, the particle will migrate more quickly if it is close to a free surface. Considering the rotational velocity, the thermophoretic particle in the vicinity of a solid wall will rotate clockwise when it approaches the plane boundary according to the positive temperature gradient, as shown in Figure 1, although the absolute value of the rotational velocity is quite small. However, the direction of the rotating particle will change to counterclockwise as the particle moves closer to the solid wall. On the other hand, the particle always will be in a counterclockwise rotation as it moves toward a free surface. Generally speaking, the influence of the boundary ef-

Table 1a. Translational and Rotational Mobilities of a Thermophoretic Sphere in the Proximity of a Plane ($k^* = 100$; $C_t^* = C_m^* = 0$)

		Solid Wall			Free Surface		
θ_T	λ	$\theta_{U,s}$	M_s	N_s	$\theta_{U,f}$	M_f	N_f
0	0.2	180	1.0000	−6.78e-5	180	1.0002	1.74e-7
	0.4	180	1.0002	−0.0003	180	1.0019	2.22e-5
	0.6	180	1.0018	0.0097	180	1.0066	0.0004
	0.8	180	1.0091	0.1001	180	1.0169	0.0028
15	0.2	165.03	0.9999	−6.55e-5	164.99	1.0003	1.68e-7
	0.4	165.23	0.9997	−0.0003	164.94	1.0020	2.15e-5
	0.6	165.86	0.9998	0.0094	164.82	1.0070	0.0004
	0.8	167.88	1.0023	0.0967	164.79	1.0174	0.0027
30	0.2	150.05	0.9997	−5.87e-5	149.99	1.0003	1.50e-7
	0.4	150.39	0.9982	−0.0002	149.90	1.0024	1.92e-5
	0.6	151.50	0.9943	0.0084	149.69	1.0082	0.0003
	0.8	155.16	0.9837	0.0867	149.64	1.0187	0.0025
45	0.2	135.06	0.9995	−4.80e-5	134.99	1.0004	1.23e-7
	0.4	135.46	0.9962	−0.0002	134.89	1.0029	1.57e-5
	0.6	136.76	0.9867	0.0069	134.64	1.0098	0.0003
	0.8	141.28	0.9577	0.0708	134.58	1.0206	0.0020
60	0.2	120.05	0.9992	−3.39e-5	119.99	1.0004	8.68e-8
	0.4	120.40	0.9942	−0.0001	119.90	1.0034	1.11e-5
	0.6	121.55	0.9791	0.0049	119.69	1.0113	0.0002
	0.8	125.76	0.9310	0.0501	119.64	1.0225	0.0014
75	0.2	105.03	0.9991	−1.76e-5	104.99	1.0005	4.49e-8
	0.4	105.23	0.9928	−7.20e-5	104.94	1.0037	5.75e-6
	0.6	105.91	0.9735	0.0025	104.82	1.0125	0.0001
	0.8	108.48	0.9109	0.0259	104.79	1.0238	0.0007
90	0.2	90	0.9990	0	90	1.0005	0
	0.4	90	0.9922	0	90	1.0039	0
	0.6	90	0.9714	0	90	1.0129	0
	0.8	90	0.9035	0	90	1.0243	0

Table 1b. Translational and Rotational Mobilities of a Thermophoretic Sphere in the Proximity of a Plane ($k^* = 100$; $C_t^* = 2C_m^* = 0.02$)

		Solid Wall			Free Surface		
θ_T	λ	$\theta_{U,s}$	M_s	N_s	$\theta_{U,f}$	M_f	N_f
0	0.2	180	1.0000	−6.34e-5	180	1.0002	4.58e-7
	0.4	180	1.0001	0.0003	180	1.0017	5.86e-5
	0.6	180	1.0017	0.0191	180	1.0058	0.0010
	0.8	180	1.0090	0.1683	180	1.0149	0.0075
15	0.2	165.03	0.9999	−6.13e-5	164.99	1.0002	4.42e-7
	0.4	165.23	0.9995	0.0003	164.95	1.0018	5.66e-5
	0.6	165.84	0.9997	0.0185	164.79	1.0063	0.0010
	0.8	167.83	1.0024	0.1626	164.58	1.0159	0.0072
30	0.2	150.05	0.9997	−5.49e-5	149.99	1.0003	3.96e-7
	0.4	150.40	0.9980	0.0002	149.91	1.0022	5.07e-5
	0.6	151.48	0.9943	0.0165	149.64	1.0077	0.0009
	0.8	155.08	0.9841	0.1458	149.27	1.0186	0.0065
45	0.2	135.06	0.9995	−4.48e-5	134.99	1.0003	3.24e-7
	0.4	135.46	0.9960	0.0002	134.89	1.0026	4.14e-5
	0.6	136.73	0.9868	0.0135	134.58	1.0095	0.0007
	0.8	141.18	0.9585	0.1190	134.17	1.0223	0.0053
60	0.2	120.05	0.9992	−3.17e-5	119.99	1.0004	2.29e-7
	0.4	120.40	0.9940	0.0001	119.91	1.0031	2.93e-5
	0.6	121.52	0.9793	0.0096	119.64	1.0113	0.0005
	0.8	125.66	0.9322	0.0842	119.28	1.0260	0.0037
75	0.2	105.03	0.9990	−1.64e-5	104.99	1.0004	1.18e-7
	0.4	105.23	0.9926	7.24e-5	104.95	1.0035	1.51e-5
	0.6	105.89	0.9738	0.0049	104.79	1.0127	0.0003
	0.8	108.42	0.9124	0.0436	104.59	1.0287	0.0019
90	0.2	90	0.9989	0	90	1.0004	0
	0.4	90	0.9920	0	90	1.0036	0
	0.6	90	0.9718	0	90	1.0132	0
	0.8	90	0.9051	0	90	1.0297	0

Table 1c. Translational and Rotational Mobilities of a Thermophoretic Sphere in the Proximity of a Plane ($k^* = 100$; $C_t^* = 2C_m^* = 0.2$)

		Solid Wall			Free Surface		
θ_T	λ	$\theta_{U,s}$	M_s	N_s	$\theta_{U,f}$	M_f	N_f
0	0.2	180	0.9998	$-6.93e$-5	180	1.0000	1.30e-7
	0.4	180	0.9985	-0.0005	180	1.0002	1.66e-5
	0.6	180	0.9956	0.0063	180	1.0008	0.0003
	0.8	180	0.9918	0.0739	180	1.0023	0.0021
15	0.2	165.03	0.9997	$-6.70e$-5	165.00	1.0000	1.25e-7
	0.4	165.28	0.9978	-0.0005	164.99	1.0002	1.60e-5
	0.6	165.98	0.9933	0.0061	164.97	1.0009	0.0003
	0.8	167.86	0.9852	0.0714	164.97	1.0023	0.0021
30	0.2	150.06	0.9995	$-6.00e$-5	150.00	1.0000	1.12e-7
	0.4	150.48	0.9961	-0.0004	149.99	1.0003	1.44e-5
	0.6	151.73	0.9870	0.0055	149.95	1.0011	0.0002
	0.8	155.13	0.9671	0.0640	149.96	1.0025	0.0018
45	0.2	135.07	0.9992	$-4.90e$-5	135.00	1.0000	9.18e-8
	0.4	135.55	0.9937	-0.0003	134.98	1.0004	1.17e-5
	0.6	137.03	0.9784	0.0045	134.94	1.0014	0.0002
	0.8	141.23	0.9417	0.0523	134.95	1.0027	0.0015
60	0.2	120.06	0.9989	$-3.47e$-5	120.00	1.0001	6.49e-8
	0.4	120.48	0.9913	-0.0002	119.99	1.0004	8.31e-6
	0.6	121.79	0.9697	0.0032	119.95	1.0016	0.0001
	0.8	125.72	0.9156	0.0370	119.96	1.0029	0.0011
75	0.2	105.03	0.9987	$-1.79e$-5	105.00	1.0001	3.36e-8
	0.4	105.28	0.9895	-0.0001	104.99	1.0005	4.30e-6
	0.6	106.05	0.9633	0.0016	104.97	1.0018	7.34e-5
	0.8	108.45	0.8960	0.0191	104.98	1.0031	0.0006
90	0.2	90	0.9986	0	90	1.0001	0
	0.4	90	0.9889	0	90	1.0005	0
	0.6	90	0.9609	0	90	1.0019	0
	0.8	90	0.8888	0	90	1.0031	0

fect, either a solid wall or a free surface, on the particle motion increases significantly as θ_T increases; that is, the boundary effect on the thermophoresis of a particle will be more notable as the particle is migrating normal to the wall than when it is parallel to the wall.

When a particle is far away from the plane boundary, the thermophoretic direction of the particle is exactly opposite to the direction of the prescribed temperature gradient. However, the presence of a plane boundary may alter the translational direction of the thermophoretic sphere. In Tables 1 and 2, when a particle is moving toward a solid wall ($e_x \cdot \nabla T_\infty < 0$, as shown in Figure 1), the influence of the boundary effects on the thermophoretic direction makes the particle move away from the plane ($\theta_U > 180° - \theta_T$), which is contrary to the case where the boundary effects are ignored ($\theta_U = 180° - \theta_T$). However, the influence of the boundary effect on the particle motion is more complicated for a free-surface situation. A particle with a small relative conductivity migrates away from the free surface, which is opposite to the case where the particle is far away from the plane. However, a free surface will push a thermophoretic particle whose thermal conductivity is large closer to the plane ($\theta_U < 180° - \theta_T$) than when the particle is isolated; here, the translational mobility of the particle is larger than 1. In general, the influence of the boundary effects on the deviation of the particle movement—for both magnitude and direction—will be more

Table 2a. Translational and Rotational Mobilities of a Thermophoretic Sphere in the Proximity of a Plane ($\lambda = 0.8$; $C_t^* = C_m^* = 0$)

k^*	θ_T	$\theta_{U,s}$	M_s	N_s	$\theta_{U,f}$	M_f	N_f
0	0	180	0.9532	-0.1219	180	0.9690	-0.0123
	15	168.68	0.9451	-0.1177	166.75	0.9650	-0.0119
	30	156.67	0.9225	-0.1055	153.09	0.9542	-0.0106
	45	143.24	0.8909	-0.0862	138.68	0.9392	-0.0087
	60	127.70	0.8580	-0.0609	123.30	0.9240	-0.0061
	75	109.73	0.8331	-0.0315	106.95	0.9126	-0.0032
	90	90	0.8238	0	90	0.9085	0
1	0	180	0.9715	-0.0313	180	0.9840	-0.0061
	15	168.26	0.9641	-0.0302	165.86	0.9820	-0.0059
	30	155.88	0.9438	-0.0271	151.51	0.9766	-0.0053
	45	142.20	0.9153	-0.0221	136.77	0.9691	-0.0043
	60	126.67	0.8859	-0.0156	121.55	0.9616	-0.0031
	75	109.06	0.8638	-0.0081	105.91	0.9561	-0.0016
	90	90	0.8555	0	90	0.9540	0
10	0	180	1.0003	0.0743	180	1.0090	0.0011
	15	167.93	0.9935	0.0718	164.98	1.0090	0.0010
	30	155.27	0.9747	0.0643	149.97	1.0092	0.0009
	45	141.42	0.9484	0.0525	134.96	1.0093	0.0008
	60	125.89	0.9213	0.0371	119.97	1.0095	0.0005
	75	108.57	0.9010	0.0192	104.98	1.0096	0.0003
	90	90	0.8934	0	90	1.0096	0
∞	0	180	1.0102	0.1034	180	1.0179	0.0031
	15	167.87	1.0035	0.0999	164.77	1.0185	0.0030
	30	155.15	0.9849	0.0896	149.60	1.0200	0.0027
	45	141.27	0.9590	0.0731	134.53	1.0221	0.0022
	60	125.75	0.9323	0.0517	119.60	1.0242	0.0015
	75	108.47	0.9122	0.0268	104.77	1.0257	0.0008
	90	90	0.9048	0	90	1.0262	0

Table 2b. Translational and Rotational Mobilities of a Thermophoretic Sphere in the Proximity of a Plane ($\lambda = 0.8$; $C_t^* = 2C_m^* = 0.02$)

k^*	θ_T	$\theta_{U,s}$	M_s	N_s	$\theta_{U,f}$	M_f	N_f
0	0	180	0.9530	-0.1190	180	0.9689	-0.0119
	15	168.68	0.9449	-0.1150	166.73	0.9650	-0.0115
	30	156.66	0.9224	-0.1031	153.06	0.9543	-0.0103
	45	143.23	0.8908	-0.0842	138.64	0.9395	-0.0084
	60	127.69	0.8580	-0.0595	123.26	0.9244	-0.0060
	75	109.73	0.8331	-0.0308	106.93	0.9132	-0.0031
	90	90	0.8239	0	90	0.9091	0
1	0	180	0.9710	-0.0321	180	0.9837	-0.0060
	15	168.26	0.9637	-0.0311	165.86	0.9818	-0.0058
	30	155.87	0.9434	-0.0278	151.51	0.9764	-0.0052
	45	142.19	0.9150	-0.0227	136.77	0.9689	-0.0043
	60	126.66	0.8856	-0.0161	121.55	0.9614	-0.0030
	75	109.05	0.8635	-0.0083	105.91	0.9559	-0.0016
	90	90	0.8553	0	90	0.9538	0
10	0	180	0.9989	0.0804	180	1.0076	0.0016
	15	167.92	0.9921	0.0777	164.97	1.0077	0.0016
	30	155.24	0.9734	0.0697	149.94	1.0079	0.0014
	45	141.38	0.9473	0.0569	134.93	1.0082	0.0012
	60	125.86	0.9204	0.0402	119.94	1.0085	0.0008
	75	108.54	0.9003	0.0208	104.97	1.0087	0.0004
	90	90	0.8928	0	90	1.0088	0
∞	0	180	1.0115	0.2150	180	1.0158	0.0106
	15	167.81	1.0049	0.2077	164.42	1.0172	0.0102
	30	155.04	0.9867	0.1862	149.00	1.0210	0.0092
	45	141.13	0.9612	0.1520	133.86	1.0261	0.0075
	60	125.61	0.9351	0.1075	119.02	1.0312	0.0052
	75	108.39	0.9155	0.0556	104.44	1.0349	0.0027
	90	90	0.9082	0	90	1.0363	0

Table 2c. Translational and Rotational Mobilities of a Thermophoretic Sphere in the Proximity of a Plane ($\lambda = 0.8$; $C_t^* = 2C_m^* = 0.02$)

k^*	θ_T	$\theta_{U,s}$	M_s	N_s	$\theta_{U,f}$	M_f	N_f
0	0	180	0.9517	−0.1020	180	0.9688	−0.0098
	15	168.68	0.9436	−0.0985	166.62	0.9652	−0.0095
	30	156.67	0.9211	−0.0883	152.86	0.9551	−0.0085
	45	143.24	0.8894	−0.0721	138.40	0.9417	−0.0070
	60	127.70	0.8566	−0.0510	123.04	0.9272	−0.0049
	75	109.74	0.8317	−0.0264	106.79	0.9167	−0.0025
	90	90	0.8225	0	90	0.9129	0
1	0	180	0.9674	−0.0381	180	0.9821	−0.0055
	15	168.27	0.9601	−0.0368	165.88	0.9801	−0.0053
	30	155.90	0.9398	−0.0330	151.54	0.9745	−0.0047
	45	142.23	0.9113	−0.0270	136.80	0.9670	−0.0039
	60	126.69	0.8819	−0.0191	121.59	0.9593	−0.0027
	75	109.08	0.8598	−0.0099	105.93	0.9537	−0.0014
	90	90	0.8515	0	90	0.9561	0
10	0	180	0.9866	0.0423	180	0.9982	0
	15	167.94	0.9799	0.0408	165.17	0.9978	0
	30	155.27	0.9613	0.0366	150.30	0.9967	0
	45	141.42	0.9354	0.0299	135.34	0.9952	0
	60	125.90	0.9087	0.0211	120.30	0.9937	0
	75	108.57	0.8886	0.0109	105.17	0.9926	0
	90	90	0.9812	0	90	0.9922	0
∞	0	180	0.9925	0.0788	0	1.0028	0.0025
	15	167.85	0.9860	0.0762	164.95	1.0029	0.0024
	30	155.11	0.9679	0.0683	149.91	1.0033	0.0021
	45	141.21	0.9426	0.0558	134.89	1.0037	0.0017
	60	125.69	0.9166	0.0394	119.91	1.0042	0.0012
	75	108.44	0.8970	0.0204	104.56	1.0045	0.0006
	90	90	0.8898	0	90	1.0046	0

significant if the plane is a solid wall than when it is a free surface.

Conclusions

The thermophoretic motion of an areosol sphere in the vicinity of a plane surface is analytically investigated in the present study. The infinite plane may be a solid wall or a free surface, and the applied temperature gradient can be in an arbitrary direction with respect to the plane where the temperature distribution is assigned to be linear. A method of reflections has been used to obtain the temperature distribution inside and outside the particle and the flow field of the surrounding fluid. Here, we have examined the mobility functions, both translational and rotational, of the thermophoretic particle in the vicinity of a plane, as well as the thickness of the thermophoretic interacting region. The results indicate that the boundary effect on the motion of a sphere due to thermophoresis can be significant when the surface-to-surface distance is small. However, this effect is still weaker than that of the motion affected by gravity.

The thermophoretic motion of a sphere normal to a solid wall always decreases as a monotonic function with λ, the ratio of the particle radius to the distance of the particle center from the wall. However, this phenomenon cannot continue if a particle with a large thermal conductivity is translating thermophoretically parallel to a conductive solid wall, because the particle can translate more quickly than when it is isolated. When the plane boundary is a free surface, the influence of the boundary effects on the particle motion may be a hindrance factor or an enhancement factor; a particle with a large thermal conductivity will migrate faster than an isolated one, whereas, a particle with a small conductivity will move slowly. Thus, in general, a free surface exerts less influence than a solid wall. Although we have assumed that the free surface remains flat, the results are valid in any circumstances where the interface deformations are small.

Acknowledgment

This research was supported by the National Science Council of the Republic of China under Grant NSC87-2214-E-146-001.

Notation

a = particle radius, m
A = coefficient defined by Eq. 7a, $m^2 \cdot s^{-1} \cdot K^{-1}$
B = coefficient defined by Eq. 12a, $m^2 \cdot s^{-1} \cdot K^{-1}$
C_1, C_2, C_3 = dimensionless coefficient defined by Eqs. 12b and 14
C_m = dimensionless coefficient accounting for the hydrodynamic slip
C_m^* = $C_m l/a$
C_s = dimensionless coefficient accounting for thermal slip
C_t = dimensionless coefficient accounting for the temperature jump
C_t^* = $C_t l/a$
D = dimensionless coefficient defined by Eq. 7b
e_r, e_θ, e_ϕ = unit vectors in spherical coordinate system
e_x, e_y, e_z = unit vectors in rectangular coordinate system
E_∞ = uniform applied temperature gradient, $K \cdot m^{-1}$
F = force exerted on a particle by the fluid, N
G = dimensionless coefficient defined by Eq. 12c
h = distance between the particle center and the plane surface, m
H = dimensionless coefficient defined by Eq. 12d
I = unit dyadic
k = thermal conductivity of the fluid, $W \cdot m^{-1} \cdot K^{-1}$
k_i = thermal conductivity of the particle, $W \cdot m^{-1} \cdot K^{-1}$
k^* = k_i/k
l = mean free path of the gas molecules, m
M = dimensionless translational mobility function defined by Eq. 10a
N = dimensionless rotational mobility function defined by Eq. 10b
p = dynamic pressure, $N \cdot m^{-2}$
r, θ, ϕ = spherical coordinate system
T = temperature distribution in the fluid, K
T_i = temperature distribution inside the particle, K
T_∞ = uniform applied temperature field, K
U = translational velocity of particle, $m \cdot s^{-1}$
U = $|U|$, $m \cdot s^{-1}$
v = velocity distribution of the fluid, $m \cdot s^{-1}$
x, y, z = rectangular coordinate system

Greek letters

δ = thickness of thermophoretic interacting region, m
$\zeta = \sqrt{(2h-x)^2 + y^2 + z^2}$, m
η = fluid viscosity, $kg \cdot m^{-1} \cdot s^{-1}$
$\lambda = a/h$
$\xi = \sqrt{(2h-x)^2 + y^2}$, m
ρ = fluid density, $kg \cdot m^{-3}$
τ = viscous stress tensor of the fluid, $N \cdot m^{-2}$
$\boldsymbol{\Omega}$ = angular velocity of particle, s^{-1}
$\Omega = |\boldsymbol{\Omega}|$, s^{-1}

Subscripts

0 = particle center
f = case for free surface
i = properties inside the particle

p = reflection from the particle
s = case for solid wall
w = reflection from the plane boundary

Superscripts

(0) = far away from the boundary
(i) = the ith reflection
(n) = case for a particle normal to a plane
(p) = case for a particle parallel to a plane

Literature Cited

Bakanov, S. P., "Thermophoresis in Gases at Small Knudsen Numbers," *Aerosol Sci. Technol.*, **15**, 77 (1991).
Brock, J. R., "On the Theory of Thermal Forces Acting on Aerosol Particles," *J. Colloid Sci.*, **17**, 768 (1962).
Chen, S. H., "Thermophoretic Deposition of a Sphere Normal to a Plane Surface," *Aerosol Sci. Technol.*, **30**, 364 (1999).
Chen, S. H., "Thermophoretic Motion of a Sphere Parallel to an Insulated Plane," *J. Colloid Interface Sci.*, **224**, 63 (2000).
Chen, S. H., and H. J. Keh, "Thermocapillary Motion of a Fluid Droplet Normal to a Plane Surface," *J. Colloid Interface Sci.*, **137**, 550 (1990).
Chen, S. H., and H. J. Keh, "Axisymmetric Thermophoretic Motion of Two Spheres," *J. Aerosol Sci.*, **26**, 429 (1995a).
Chen, S. H., and H. J. Keh, "Axisymmetric Motion of Two Spherical Particles with Slip Surfaces," *J. Colloid Interface Sci.*, **171**, 63 (1995b).
Chen, S. H., and H. J. Keh, "Axisymmetric Thermophoresis of Multiple Aerosol Spheres," *Aerosol Sci. Technol.*, **24**, 21 (1996).
Friedlander, S. K., *Smoke, Dust and Haze*, Wiley, New York (1977).
Happel, J., and H. Brenner, *Low Reynolds Number Hydrodynamics*, Nijhoff, Dordrecht, The Netherlands (1983).
Keh, H. J., and S. H. Chen, "Particle Interactions in Thermophoresis," *Chem. Eng. Sci.*, **50**, 3395 (1995).
Keh, H. J., and S. H. Chen, "Thermophoresis of an Arbitrary Three-Dimensional Array of N Interacting Arbitrary Spheres," *J. Aerosol Sci.*, **27**, 1035 (1996a).
Keh, H. J., and S. H. Chen, "The Motion of a Slip Spherical Particle in an Arbitrary Stokes Flow," *Eur. J. Mech., B/Fluids*, **15**, 791 (1996b).
Keh, H. J., and S. H. Chen, "Low-Reynolds-Number Hydrodynamic Interactions in an Suspension of Spherical Particles with Slip Surfaces," *Chem. Eng. Sci.*, **52**, 1789 (1997).
Keh, H. J., and J. L. Yu, "Migration of Aerosol Spheres under the Combined Action of Thermophoretic and Gravitational Effects," *Aerosol Sci. Technol.*, **22**, 250 (1995).
Kennard, E. H., *Kinetic Theory of Gases*, McGraw-Hill, New York (1938).
Leong, K. H., "Thermophoresis and Diffusiophoresis of Large Aerosol Particles of Different Shapes," *J. Aerosol Sci.*, **15**, 511 (1984).
Montassier, N., D. Boulaud, and A. Renoux, "Experimental Study of Thermophoretic Particle Deposition in Laminar Tube Flow," *J. Aerosol Sci.*, **22**, 677 (1991).
Sasse, A. G. B. M., W. W. Nazaroff, and A. J. Gadgil, "Particle Filter Based on Thermophoretic Deposition from Natural Convection Flow," *Aerosol Sci. Technol.*, **20**, 227 (1994).
Talbot, L., R. K. Cheng, R. W. Scheffer, and D. R. Willis, "Thermophoresis of Particles in a Heated Boundary Layer," *J. Fluid Mech.*, **101**, 737 (1980).
Waldmann, L., and K. H. Schmitt, "Thermophoresis and Diffusiophoresis of Aerosols," *Aerosol Science*, C. N. Davies, ed., Academic Press, New York (1966).
Weinberg, M. C., "Thermophoretic Efficiency in Modified Chemical Vapor Deposition Process," *J. Amer. Ceram. Soc.*, **65**, 81 (1982).
Williams, M. M. R., and S. K. Loyalka, *Aerosol Science: Theory and Practice, with Special Applications to the Nuclear Industry*, Pergamon Press, Oxford (1991).
Ye, Y., D. Y. H. Pui, B. Y. H. Liu, S. Opiolka, S. Blumhorst, and H. Fissan, "Thermophoretic Effect of Particle Deposition on a Free Standing Semiconductor Wafer in a Clean Room," *J. Aerosol Sci.*, **22**, 63 (1991).

Appendix: Thermophoresis of a Sphere Parallel to a Conductive Plane

Here, we consider the thermophoretic motion of an aerosol sphere parallel to a thermally conductive plane by using a method of reflections. Obviously, the unperturbed temperature gradient gives

$$\boldsymbol{U}^{(0)} = U^{(0)}\boldsymbol{e}_z, \tag{A1a}$$

$$\boldsymbol{\Omega}^{(0)} = \boldsymbol{0}, \tag{A1b}$$

with $U^{(0)} = AE_\infty$.

The solution for the first reflected temperature and velocity fields from the particle that satisfies the appropriate boundary conditions at the particle surface is furnished by (Keh and Chen, 1995)

$$T_p^{(1)} = Ga^3E_\infty zr^{-3}, \tag{A2a}$$

$$\boldsymbol{v}_p^{(1)} = \frac{1}{2}a^3U^{(0)}\left[3xzr^{-5}\boldsymbol{e}_x + 3yzr^{-5}\boldsymbol{e}_y + (3z^2 - r^2)r^{-5}\boldsymbol{e}_z\right], \tag{A2b}$$

where $r\ (=\sqrt{x^2+y^2+z^2})$ is the radial component in the spherical coordinates; G is defined by Eq. 12c; $\boldsymbol{e}_x$, $\boldsymbol{e}_y$, and $\boldsymbol{e}_z$ are the unit vectors in the rectangular coordinates.

The boundary conditions for the succeeding reflected fields from the plane surface are

$$x = h \qquad T_w^{(1)} = -T_p^{(1)}, \tag{A3a}$$

$$\boldsymbol{v}_w^{(1)} = -\boldsymbol{v}_p^{(1)} \qquad \text{(solid wall)}$$

$$\left.\begin{aligned} \boldsymbol{e}_x\cdot\boldsymbol{v}_w^{(1)} &= -\boldsymbol{e}_x\cdot\boldsymbol{v}_p^{(1)} \\ \boldsymbol{e}_x\boldsymbol{e}_z:\boldsymbol{\tau}_w^{(1)} &= -\boldsymbol{e}_x\boldsymbol{e}_z:\boldsymbol{\tau}_p^{(1)} \end{aligned}\right\} \quad \text{(free surface)} \tag{A3b}$$

$$x \le h, y^2+z^2 \to \infty \qquad T_w^{(0)} \to 0, \tag{A3c}$$

$$\boldsymbol{v}_w^{(1)} \to \boldsymbol{0}, \tag{A3d}$$

where $\tau_p^{(1)}$ and $\tau_w^{(1)}$ are deviatoric stress tensors corresponding to $\boldsymbol{v}_p^{(1)}$ and $\boldsymbol{v}_w^{(1)}$, respectively.

The solution for $T_w^{(1)}$ is obtained by applying complex Fourier transforms on y and z in Eqs. 2a, A3a, and A3c, with the result

$$T_w^{(1)} = -Ga^3E_\infty z\zeta^{-3}, \tag{A4}$$

where $\zeta = \sqrt{(2h-x)^2 + y^2 + z^2}$. This reflected temperature field can be seen to come from the reflection of the imposed field $E_\infty \boldsymbol{e}_z$ from a fictitious sphere equal in size to the actual sphere, its location being at the mirror-image position of the actual sphere with respect to the plane $x = h$ (that is, at $x = 2h$, $y = 0$, $z = 0$).

The general solution to the Stokes equation (Eq. 4), which is established by Faxen (Happen and Brenner, 1983), is

$$v_x = \frac{1}{4\pi^2}\int_{-\infty}^{\infty}\int_{-\infty}^{\infty} e^{i(\alpha y + \beta z) + qx}\left[g_2 - i\beta x q^{-1} g_1 + i\beta q^{-1} g_3(1 - qx)\right]\, d\alpha\, d\beta, \tag{A5a}$$

$$v_y = \frac{1}{4\pi^2}\int_{-\infty}^{\infty}\int_{-\infty}^{\infty} e^{i(\alpha y+\beta z)+qx} i\alpha\left[q^{-1}g_2 + i\beta q^{-3}g_1(1-qx) - i\beta x q^{-1}g_3\right] d\alpha\, d\beta, \quad \text{(A5b)}$$

$$v_x = \frac{1}{4\pi^2}\int_{-\infty}^{\infty}\int_{-\infty}^{\infty} e^{i(\alpha y+\beta z)+qx}\left[i\beta q^{-1}g_2 + 2q^{-1}g_1 - \beta^2 q^{-3}g_1(1-qx) + \beta^2 x q^{-1}g_3\right] d\alpha\, d\beta, \quad \text{(A5c)}$$

and

$$p = \frac{\eta}{\pi}\int_{-\infty}^{\infty}\int_{-\infty}^{\infty} e^{i(\alpha y+\beta z)+qx} i\beta q^{-1}(-g_1 - qg_3)\, d\alpha\, d\beta. \quad \text{(A6)}$$

Here, $i=\sqrt{-1}$; α and β are dummy variables of integration; $q=\sqrt{\alpha^2+\beta^2}$. The quantities g_1, g_2, and g_3 may be any functions of α and β. This representation is valuable because it is naturally adapted to satisfy boundary conditions on both spherical and plane boundaries. With knowledge of $\boldsymbol{v}_p^{(1)}$ and $T_p^{(1)}$, $\boldsymbol{v}_w^{(1)}$ can be found by fitting the boundary conditions given in Eqs. A3b and A3d with the general solution (Eq. A5), which results in

$$\boldsymbol{v}_{ws}^{(1)} = -\frac{1}{2}a^3U^{(0)}\Big\{3\left[xz\zeta^{-5} + 10(h-x)(2h-x)^2 z\zeta^{-7}\right]\boldsymbol{e}_x + 3\left[yz\zeta^{-5} - 10(h-x)(2h-x)yz\zeta^{-7}\right]\boldsymbol{e}_y + \left[6(h-x)(2h-x)(\zeta^{-5} - 5z^2\zeta^{-7}) - \zeta^{-3} + 3z^2\zeta^{-5}\right]\boldsymbol{e}_z\Big\}, \quad \text{(A7a)}$$

$$\boldsymbol{v}_{wf}^{(1)} = -\frac{1}{2}a^3U^{(0)}\left[3(2h-x)z\zeta^{-5}\boldsymbol{e}_x - 6yz\zeta^{-5}\boldsymbol{e}_y + (\zeta^{-3} - 3z^2\zeta^{-5})\boldsymbol{e}_z\right], \quad \text{(A7b)}$$

where the subscripts s and f denote the cases for a solid wall and for a free surface, respectively. After substituting $T_w^{(1)}$ and $\boldsymbol{v}_{ws}^{(1)}$ or $\boldsymbol{v}_{wf}^{(1)}$ into Eq. 6, one has

$$\boldsymbol{U}_s^{(1)} = \left[-\frac{1}{8}(1+G)\lambda^3 + \frac{3}{32}D\lambda^5\right]\boldsymbol{U}^{(0)}, \quad \text{(A8a)}$$

$$a\boldsymbol{\Omega}_s^{(1)} = \frac{3}{64}\lambda^4\boldsymbol{e}_x \times \boldsymbol{U}^{(0)}, \quad \text{(A8b)}$$

$$\boldsymbol{U}_f^{(1)} = \left[-\frac{1}{16}(1+2G)\lambda^3 + 0\lambda^5\right]\boldsymbol{U}^{(0)}, \quad \text{(A8c)}$$

$$a\boldsymbol{\Omega}_f^{(1)} = \boldsymbol{0}, \quad \text{(A8d)}$$

where D is defined by Eq. 7b.

Again, the solution for the second reflected temperature and velocity fields can be obtained from the general solution derived by Keh and Chen (1995) by replacing T_A and $\boldsymbol{v}_A$ by $T_w^{(1)}$ and $\boldsymbol{v}_{ws}^{(1)}$ (or $\boldsymbol{v}_{wf}^{(1)}$). Thus, one can obtain

$$T_p^{(2)} = \frac{1}{8}G^2\lambda^3a^3E_\infty zr^{-3} - \frac{3}{8}GH\lambda^4a^4E_\infty xzr^{-5}, \quad \text{(A9a)}$$

$$\boldsymbol{v}_{ps}^{(2)} = -\frac{1}{16}Ga^3\lambda^3U^{(0)}\left[3xzr^{-5}\boldsymbol{e}_x + 3yzr^{-5}\boldsymbol{e}_y + (3z^2r^{-5} - r^{-3})\boldsymbol{e}_z\right] - \frac{9}{32}\left(4\frac{B}{A}G - 5C_1\right)a^2\lambda^4U^{(0)}\left(x^2zr^{-5}\boldsymbol{e}_x + xyzr^{-5}\boldsymbol{e}_y + xz^2r^{-5}\boldsymbol{e}_z\right) + \frac{3}{64}C_2a^2\lambda^4U^{(0)}\left(zr^{-3}\boldsymbol{e}_x - xr^{-3}\boldsymbol{e}_z\right) - \frac{3}{32}\left(4\frac{B}{A}G - 3C_3\right)a^4\lambda^4U^{(0)}\left[(zr^{-5} - 5x^2zr^{-7})\boldsymbol{e}_x - 5xyzr^{-7}\boldsymbol{e}_y + (xr^{-5} - 5xz^2r^{-7})\boldsymbol{e}_z\right], \quad \text{(A9b)}$$

$$\boldsymbol{v}_{pf}^{(2)} = -\frac{1}{16}Ga^3\lambda^3U^{(0)}\left[3xzr^{-5}\boldsymbol{e}_x + 3yzr^{-5}\boldsymbol{e}_y + (3z^2r^{-5} - r^{-3})\boldsymbol{e}_z\right] - \frac{3}{32}\left(12\frac{B}{A}G - 5C_1\right)a^2\lambda^4U^{(0)}\left(x^2zr^{-5}\boldsymbol{e}_x + xyzr^{-5}\boldsymbol{e}_y + xz^2r^{-5}\boldsymbol{e}_z\right) - \frac{3}{32}\left(4\frac{B}{A}G - C_3\right)a^4\lambda^4U^{(0)}\left[(zr^{-5} - 5x^2zr^{-7})\boldsymbol{e}_x - 5xyzr^{-7}\boldsymbol{e}_y + (xr^{-5} - 5xz^2r^{-7})\boldsymbol{e}_z\right], \quad \text{(A9c)}$$

where coefficients B, C_1, C_2, C_3, and H are defined by Eqs. 12 and 14.

Following the same procedure of derivation as in Eqs. A4 and A7, one can obtain the results of $T_w^{(2)}$ and $\boldsymbol{v}_{ws}^{(2)}$ or $\boldsymbol{v}_{wf}^{(2)}$, which are in the forms of higher order λ,

$$T_w^{(2)} = \frac{1}{8}G^2a^3\lambda^3E_\infty z\zeta^{-3} + \frac{3}{8}GHa^4\lambda^4E_\infty(2h-x)z\zeta^{-5}, \quad \text{(A10a)}$$

$$\boldsymbol{v}_{ws}^{(2)} = \frac{1}{16}Ga^3\lambda^3U^{(0)}\Big\{3\left[xz\zeta^{-5} + 10(h-x)(2h-x)^2z\zeta^{-7}\right]\boldsymbol{e}_x + 3\left[yz\zeta^{-5} - 10(h-x)(2h-x)yz\zeta^{-7}\right]\boldsymbol{e}_y + \left[6(h-x)(2h-x)(\zeta^{-5} - 5z^2\zeta^{-7}) - \zeta^{-3} + 3z^2\zeta^{-5}\right]\boldsymbol{e}_z\Big\} + \frac{9}{32}\left(4\frac{B}{A}G - 5C_1\right)a^2\lambda^4U^{(0)}\Big\{\left[10h(h-x)(2h-x)^2z\zeta^{-7} - 2h(h-x)z\zeta^{-5} + (2h-x)xz\zeta^{-5}\right]\boldsymbol{e}_x + \left[(2h-x)yx\zeta^{-5} - 10h(h-x)(2h-x)yz\zeta^{-7}\right]\boldsymbol{e}_y + \left[(2h-x)z^2\zeta^{-5} + 2h(h-x)(2h-x)(5\xi^2\zeta^{-7} - 4\zeta^{-5}\right]\boldsymbol{e}_z\Big\}$$

$$-\frac{3}{64}C_2a^2\lambda^4U^{(0)}\{[6(h-x)(2h-x)z\zeta^{-5}]e_x$$

$$-6(h-x)yz\zeta^{-5}e_y-[x\zeta^{-3}+6(h-x)z^2\zeta^{-5}]e_z\}$$

$$+\frac{3}{32}\left(4\frac{B}{A}G-3C_3\right)a^4\lambda^4U^{(0)}\{[z\zeta^{-5}$$

$$+5(4h-5x)(2h-x)z\zeta^{-7}-70(h-x)(2h-x)^3z\zeta^{-9}]e_x$$

$$-10[(h-x)yz\zeta^{-7}-7(h-x)(2h-x)^2yz\zeta^{-9}]e_y$$

$$-[4(4h-3x)\zeta^{-5}-5(4h-3x)\xi^2\zeta^{-7}$$

$$-60(h-x)(2h-x)^2\zeta^{-7}+70(h-x)(2h-x)^2\xi^2\zeta^{-9}]e_z\}, \quad \text{(A10b)}$$

$$v_{wf}^{(2)}=\frac{1}{16}Ga^3\lambda^3U^{(0)}[3(2h-x)z\zeta^{-5}e_x-6yz\zeta^{-5}e_y$$

$$+(\zeta^{-3}-3z^2\zeta^{-5})e_z]+\frac{3}{32}\left(12\frac{B}{A}G\right.$$

$$\left.-5C_1\right)a^2\lambda^4U^{(0)}[(2h-x)^2z\zeta^{-5}e_x$$

$$-2(2h-x)yz\zeta^{-5}e_y-(2h-x)z^2\zeta^{-5}e_z]$$

$$+\frac{3}{64}\left(8\frac{B}{A}G-3C_3\right)a^4\lambda^4U^{(0)}\{[z\zeta^{-5}$$

$$-5(2h-x)^2z\zeta^{-7}]e_x+5(2h-x)yz\zeta^{-7}e_y+[4(2h-x)\zeta^{-5}$$

$$-5(2h-x)\xi^2\zeta^{-7}]e_z\}, \quad \text{(A10c)}$$

where $\xi=\sqrt{(2h-x)^2+y^2}$. Substituting $T_w^{(2)}$ and $v_{ws}^{(2)}$ or $v_{wf}^{(2)}$ into Eq. 6, the second reflected velocities are

$$U_s^{(2)}=\left[\frac{1}{256}\left(4G+4G^2+36\frac{B}{A}G-45C_1\right)\lambda^6\right.$$

$$+\frac{3}{2{,}048}\left(16GH-48\frac{B}{A}G-8DG-44\frac{B}{A}DG\right.$$

$$\left.\left.+55C_1D+3C_2D+36C_3\right)\lambda^8\right]U^{(0)}, \quad \text{(A11a)}$$

$$a\Omega_s^{(2)}=\left[-\frac{3}{1{,}024}\left(8G+384\frac{B}{A}G-30C_1-5C_2\right)\lambda^7\right.$$

$$\left.+\frac{3}{128}\left(4\frac{B}{A}G-3C_3\right)\lambda^9\right]e_x\times U^{(0)}, \quad \text{(A11b)}$$

$$U_f^{(2)}=\left[\frac{1}{128}(G+2G^2)\lambda^6+\frac{1}{1{,}024}\left(24GH+24\frac{B}{A}G\right.\right.$$

$$\left.\left.-24\frac{B}{A}DG+10C_1D-9C_3\right)\lambda^8\right]U^{(0)}, \quad \text{(A11c)}$$

$$a\Omega_f^{(2)}=\left[-\frac{3}{512}\left(12\frac{B}{A}G-5C_1\right)\lambda^7+0\lambda^9\right]e_x\times U^{(0)}. \quad \text{(A11d)}$$

With the addition of Eqs. A2, A8 and A11, the particle velocity can be expressed as

$$U_s=\left[1-\frac{1}{8}(1+G)\lambda^3+\frac{3}{32}D\lambda^5+\frac{1}{256}\left(4G+4G^2\right.\right.$$

$$\left.+36\frac{B}{A}G-45C_1\right)\lambda^6+\frac{3}{2{,}048}\left(16GH-48\frac{B}{A}G-8DG\right.$$

$$\left.-44\frac{B}{A}DG+55C_1D+3C_2D+36C_3\right)\lambda^8$$

$$\left.+O(\lambda^9)\right]U^{(0)}, \quad \text{(A12a)}$$

$$a\Omega_s=\left[\frac{3}{64}\lambda^4+0\lambda^6-\frac{3}{1{,}024}\left(8G+384\frac{B}{A}G-30C_1-5C_2\right)\lambda^7\right.$$

$$\left.+\frac{3}{128}\left(4\frac{B}{A}G-3C_3\right)\lambda^9+O(\lambda^{10})\right]e_x\times U^{(0)}, \quad \text{(A12b)}$$

for the thermophoretic motion parallel to a solid wall, and

$$U_f=\left[1-\frac{1}{16}(1+2G)\lambda^3+0\lambda^5+\frac{1}{128}(G+2G^2)\lambda^6\right.$$

$$+\frac{1}{1{,}024}\left(24GH+24\frac{B}{A}G-24\frac{B}{A}DG+10C_1D-9C_3\right)\lambda^8$$

$$\left.+O(\lambda^9)\right]U^{(0)}, \quad \text{(A12c)}$$

$$a\Omega_f=\left[0\lambda^4+0\lambda^6-\frac{3}{512}\left(12\frac{B}{A}G-5C_1\right)\lambda^7\right.$$

$$\left.+0\lambda^9+O(\lambda^{10})\right]e_x\times U^{(0)}, \quad \text{(A12d)}$$

for the movement in the vicinity of a free surface. The $O(\lambda^9)$ and $O(\lambda^{10})$ interactions for translational and rotational velocities, respectively, in Eq. A12 can be obtained by more detailed calculations of $T_w^{(3)}$ and $v_w^{(3)}$ and their derivatives at the position at the center of the particle, but the numerical significance would be small except when the gap between the surfaces of the particle and plane approached zero.

Manuscript received Mar. 29, 1999, and revision received Apr. 17, 2000.